



Inorganic Nano-Adsorbents for the Removal of Heavy Metals and Arsenic: A Review

Journal:	<i>RSC Advances</i>
Manuscript ID:	RA-REV-02-2015-002714.R1
Article Type:	Review Article
Date Submitted by the Author:	12-Mar-2015
Complete List of Authors:	Ray, Phoebe; University of New Orleans, Shipley, Heather; University of Texas at San Antonio, Civil and Environmental Engineering

Inorganic Nano-Adsorbents for the Removal of Heavy Metals and Arsenic: A Review

Phoebe Zito Ray and Heather J. Shipley,^{1†}*

*University of New Orleans, Dept. of Chemistry, 2000 Lakeshore Dr., New Orleans, LA 70148

†University of Texas-San Antonio, Dept. of Civil and Environmental Engineering, One UTSA
Circle, San Antonio, TX 78249

Abstract

Adsorption is widely popular for removal of heavy metals due to its low cost, efficiency, and simplicity. The focus of this review will be the use of inorganic adsorbents engineered at the nanoscale. The applicability of iron oxide (hematite, magnetite and maghemite), carbon nanotubes (CNT), and metal oxide based (Ti, Zn) and polymeric nanoadsorbents are examined. The advantages and limitations of the type of nanoadsorbent and its functionality are evaluated. Current developments and next generation adsorbents are also reviewed. Finally, scopes and limitations of these adsorbents will be addressed while investigating the types of metal ions that are harmful.

1 Introduction

The anthropogenic release of heavy metals into the environment is becoming a global epidemic.¹

² These species can enter natural waters through release of wastewater, industrial activity³ and domestic effluents.^{4,5} In 1988, Nriagu and Pacyna published a quantitative assessment of

¹ To whom correspondence may be addressed Heather J. Shipley One UTSA Circle San Antonio, TX 78249, fax 210-458-6475, heather.shipley@utsa.edu

21 emission studies in Western Europe, the United States and the Soviet Union.⁶ They concluded
22 that “mankind” was the biggest contributor in the deployment of trace metals into the
23 environment.⁶ Almost 30 years later, the release of heavy metals into the environment continues
24 to be a worldwide issue. Although anthropogenic sources cause much of the environmental
25 pollution, heavy metals can also be introduced into the environment through natural sources.
26 Natural sources of heavy metals can include weathering, erosion from rock and soil, rainwater.⁷
27 Natural sources of heavy metal release into the environment are dominated by interfaces between
28 solids, liquids and gases.⁸ These interfacial interactions, especially between natural solids (rock)
29 and aqueous solutions (water), can contribute to the release or accumulation of heavy metals into
30 the environment.⁸ These processes occur through mineral dissolution, precipitation, and
31 sorption/desorption of chemical species, which can evolve to become pollutants in soils and
32 groundwater.⁸ This combination of natural and anthropogenic sources can cause heavy metals to
33 accumulate and as a result, have toxic effects to humans and other living organisms.⁹⁻¹¹
34 According to the United States Environmental Protection Agency (EPA), the most toxic heavy
35 metals include arsenic, copper, mercury, nickel, cadmium, lead and chromium.¹² The ingestion
36 of these metals can cause a number of health issues, such as severe developmental and
37 neurological disorders over relatively short time periods or even death.¹²

38 Currently, the most common methods to remove heavy metals from water and
39 wastewater are ion exchange,¹³⁻¹⁵ reverse osmosis,^{16, 17} chemical precipitation,¹⁸ electrochemical
40 treatment¹⁹⁻²¹, membrane filtration²², floatation²³, and adsorption.¹ The most recognized method
41 for heavy metal treatment is adsorption.

42 The many advantages of adsorption are that it is versatile, it does not require high
43 amounts of energy, large amounts of water or additional chemicals.^{24, 25} In developing countries

44 where access to large amounts of power and financial resources can be an issue, this simple and
45 cheap process would be a viable option. The mechanistic process of adsorption allows versatility
46 in the design and use of the adsorbent. The two most common methods used for adsorption are
47 the batch method and column or flow method. The batch method is where the adsorbate is added
48 to the sorbent in an aqueous suspension under continuous mixing or agitation.²⁶ A column or
49 flow method uses a continuous flow of liquid through a fixed bed of the adsorbent. The flow of
50 the liquid through the fixed bed is set at a fixed rate. The flow method is typically applied in
51 industrial settings.

52 In order to measure and classify adsorption systems, isotherms are generated. Isotherms
53 are curves that are based on computational expressions that follow the Gibbs adsorption
54 isotherm, which predicts the thermodynamic conditions for interfacial systems.²⁷ The nature of
55 the curve and the initial slope can be observed and used to give the relationship between solute
56 adsorption mechanisms at the surface of the solid, the pressure, and the type of adsorption
57 isotherm to classify the system.²⁸ An isotherm can be used to describe and identify the
58 mechanism of adsorption between the solute and the substrate surface as well as the adsorption
59 capacity of adsorbent.²⁸ There are many adsorption isotherms (Adamson and Gast 1997), the two
60 most commonly observed types of isotherms are Langmuir and Freundlich. Generally, the curve
61 generated from the Langmuir isotherm shows an initial slope dependent on the rate of change of
62 available sites on the particle with increasing solute adsorbing to the sites.²⁸ As more solute is
63 adsorbed, there is a decreased chance that additional species can find an adsorption site, and the
64 curve will form a plateau.²⁸

65 The Freundlich equation is similar to the Langmuir equation in that it produces a
66 graphical representation of the amount of solute adsorbed on the surface of the substrate

67 (adsorbent), at which this sorption occurs. The difference, however, is that the Langmuir
68 adsorption isotherm gives the amount of solute adsorbing on the external surface of the adsorbent
69 in the form of a monolayer.²⁹ Therefore, in theory, it represents the equilibrium distribution of
70 ions between the solid and liquid phase.²⁹ The Freundlich adsorption isotherm empirically
71 describes the adsorption characteristics for the liquid-solid interface.²⁹

72 Other key parameters addressed were those that control adsorption of a solute onto an
73 adsorbent are pH, temperature, concentration of the solute and adsorbent, and the surface area
74 available on the surface of the adsorbent. The articles that are discussed in this review provide a
75 comprehensive analysis giving details of each of the aforementioned parameters. One should
76 also mention that the articles presented in this review provided extensive characterization of their
77 nanomaterials using transmission electron microscopy (TEM), scanning electron microscopy
78 (SEM), x-ray diffraction (XRD), X-ray photoelectron spectroscopy (XPS), thermogravimetric
79 analysis (TGA), Fourier transform infrared spectroscopy (FTIR), Brunauer-Emmett-Teller (BET)
80 theory, and other techniques. Though these techniques are important and were accounted for,
81 they will not be mentioned in this review. The main focus will be on the performance of the
82 inorganic nanoadsorbents when they are in contact with heavy metal ions.

83 Adsorption is widely popular for removal of heavy metals due to its low cost, efficiency,
84 and simplicity.³⁰ According to a review article published by Bailey *et al*, to consider an
85 adsorbent to be “low cost” it has to be abundant in nature, originated from waste or by-products,
86 or is minimally processed.³¹ Adsorbents can be purchased commercially, engineered at the
87 nanoscale, or prepared from agricultural waste as raw materials. There have been many
88 published methods in the last decade that focus on using materials such as agricultural raw
89 materials³²⁻³⁹, biomaterials, polymers, metal oxides, and others to remove heavy metals from

90 water.^{40, 41, 42} The focus of this review will be the use of inorganic adsorbents engineered at the
91 nanoscale. Nanomaterials are generally defined as having at least one dimension in the range of
92 1-100 nm.⁴² A nanomaterial possesses certain properties and morphologies that make it a great
93 candidate as an adsorbent for removing heavy metals from contaminated waters, including
94 enhanced surface area in comparison to bulk particles. The larger surface area per mass allows
95 more sites for surface chemistry. They also have the ability to be tuned with different chemical
96 species to increase their functionality toward specific targets.⁴³ In the case for heavy metal
97 removal, particles can be surface functionalized to increase the affinity for a specific ion. The
98 research reported in this review covers pertinent literature from 2004-2014 focusing on the
99 removal of heavy metal ions in synthetic solutions, natural waters and wastewater.

100 This article will provide a thorough review covering the types of inorganic
101 nanoadsorbents and the type of metal ions being removed. The applicability of iron oxide
102 (hematite, magnetite and maghemite), carbon nanotubes (CNT), and metal oxide based (Ti, Mn,
103 Zn) and polymeric nanoadsorbents are examined. The advantages and limitations of the type of
104 nanoadsorbent and its functionality are evaluated. Current developments and next generation
105 adsorbents are also reviewed. Finally, scopes and limitations of these adsorbents will be
106 addressed while investigating the types of metal ions that are harmful.

107 **2 Inorganic Nano-Adsorbents**

108 109 2.1 Heavy Metals being removed

110 A number of simple or complex metal ions and species pose serious health threats to humans
111 and other animals and must be removed from the environment, including arsenic (As), cadmium
112 (Cd), chromium (Cr), cobalt (Co), copper (Cu), lead (Pb), mercury (Hg), nickel (Ni), and Zinc
113 (Zn). These metals, often in the form of complex ions, are present due to the erosion of natural

114 materials and anthropogenic sources (industrial wastewater).¹² In the last ten years, many
115 research groups have investigated the use of nanoparticles for heavy metal removal due to their
116 high surface area and ability for their surfaces to be functionalized in order to increase efficiency
117 or adsorption capability.⁴⁴ Inorganic nanoadsorbents that will be covered in this review include
118 magnetic nanoparticles, carbon nanotubes (CNT), metal-oxide based nanoparticles, and
119 polymeric nanoadsorbents.

120 2.2 Iron Oxide Nanomaterials

121 The growing interest in the use of iron oxide nanoparticles for heavy metal clean-up is due to
122 their simplicity and resourcefulness. The three phases of iron oxide discussed in this article, are
123 the magnetic phase-magnetite (Fe_3O_4) and maghemite ($\gamma\text{-Fe}_2\text{O}_4$) and non-magnetic, hematite ($\alpha\text{-}$
124 Fe_2O_3). These phases can be synthesized using a wide range of techniques from sol-gel, thermal
125 decomposition, hydrothermal, solvothermal, and chemical vapor deposition. They can also be
126 synthesized into different structural morphologies like nanochains,⁴⁵ flowers,⁴⁶ cauliflower-like
127 structures,⁴⁷ nanotubes,⁴⁸ nanorods³⁰ and nanoparticles.³³ This article will review nanoparticles
128 made of these three phases of iron oxide, with varying sizes and experimental parameters that
129 were used during the adsorption process.

130 2.2.1 Magnetite (Fe_3O_4) and Maghemite ($\gamma\text{-Fe}_2\text{O}_4$)

131
132 It is a challenge to separate and recover sorbent materials from water that has become
133 contaminated. Magnetic versions of iron oxide sorbent nanomaterials offer a viable solution to
134 collect and remove toxic species. This advantage is because they can be easily removed from the
135 system by simply applying an external magnetic field. There have been many reports on the use
136 of MNPs for cleanup of heavy metals including arsenic,⁴⁹ chromium,⁴⁹⁻⁵¹ cobalt,⁵² copper, lead,⁵¹
137 and nickel⁵² from aqueous synthetic solutions and natural water systems. The experimental

138 conditions for the adsorption of these ions onto the MNPs vary. However, the highlights covered
139 are the morphology of the nanoadsorbent, how it was synthesized, the adsorption efficiency,
140 what type of heavy metal ions were being removed and the type of sample matrix, i.e. “natural
141 water samples” or lab prepared.

142 2.2.1.1 Nanoparticles, Nanotubes, rods and other morphologies

143
144 Magnetite nanoparticles are ideal adsorbents for arsenic species due to their affinity for
145 arsenate and arsenite and simple removal from solution using low magnetic fields.⁵³ Shipley *et*
146 *al.* conducted arsenic adsorption studies along with examining the effect of common aquatic
147 contaminants (sulfate, silica, calcium, bicarbonate, dissolved organic matter, phosphate,
148 magnesium and iron). Adsorption experiments took place in a sealed vessel containing 100 µg/L
149 As (V) with 0.5 g/L magnetite nanoparticles in Houston tap water and 39 µg/L total arsenic
150 contaminated groundwater from Brownsville, TX with 0.5 g/L magnetite nanoparticles. About
151 83 µg/L of arsenate was adsorbed within one hour from the spiked Houston tap water. For the
152 arsenic contaminated groundwater, the amount of arsenic in solution was reduced to 10 µg/L in
153 less than 10 mins and 5 µg/L within one hour. The results correlated well with the Langmuir
154 isotherm model and demonstrated that magnetite nanoparticles have the ability to remove arsenic
155 species from water in the presence of other species such as phosphates and carbonates. The use
156 of a representative wastewater and drinking water samples exemplifies the application for
157 household use; however, the authors note that more research is needed to apply toward industrial
158 applications.⁵³

159 In 2013, Roy *et al* removed Cu (II), Zn (II) and Pb (II) from water using maghemite
160 nanotubes (MHNT).⁴⁸ They synthesized the maghemite nanotubes using a template free
161 microwave irradiation and determined adsorption kinetics.⁵⁴ In order to evaluate the adsorption

162 capacity of the metal ion to the MHNTs, Langmuir and Freundlich isotherm models were
163 applied.⁵⁴ The Langmuir isotherm showed better correlation to the observed behavior for the
164 adsorption of the metals onto the MHNTs than the Freundlich model.⁴⁸ At an initial
165 concentration of 100 mg/L, favorable adsorption was observed for all metal ions tested in this
166 study (Table 1). In 2013, Karami reported the use of magnetite nanorods for heavy metal ion
167 removal from lab prepared aqueous solutions containing Fe^{2+} , Pb^{2+} , Zn^{2+} , Ni^{2+} , Cd^{2+} , and Cu^{2+}
168 ions.³⁰ They previously presented a method for preparation of uniform magnetite nanorods via
169 pulsed electrosynthesis method.⁵⁵ Adsorption/desorption studies were carried out and fit to
170 isotherms in order to determine the capacity of the magnetite nanorods. Both Langmuir and
171 Freundlich isotherm models were applied, and the Langmuir isotherm demonstrated a better fit to
172 the data.³⁰ The nanorods, due to their high surface area, showed increased metal ion adsorption
173 at pH 5.5, representative of natural groundwater.³⁰ A comparison between the magnetite
174 nanorods with the maghemite nanotubes synthesized by Roy *et al* was conducted.^{30, 54}
175 Furthermore, the adsorption capacities of the nanorods versus the nanotubes using solutions
176 containing Cu^{2+} , Zn^{2+} , and Pb^{2+} were compared.³⁰ The nanorods showed higher adsorption
177 capacity for Zn^{2+} and Pb^{2+} but lower adsorption capacity for Cu^{2+} when compared to the
178 nanotubes.³⁰ Karami attributed the lower Cu^{2+} adsorption due to the morphology of the
179 nanorods.³⁰ They attributed the adsorption mechanism for the nanorods to electrostatic forces
180 between the negatively charged adsorbent and positive metal ions.³⁰ After adsorption
181 experiments, the nanorods were removed via low magnetic field.³⁰ Although both groups created
182 a representative sample solution in the lab, they did not test their nanoadsorbents using natural
183 water samples. In a natural water sample, there are many other types of ions present that can
184 compete for adsorption onto the particle surface. In addition, natural organic matter (NOM) can

185 coordinate metals and change their adsorption behavior. To really determine if the
186 nanoadsorbent will be applicable outside the laboratory and in practical applications, it must be
187 tested accordingly.

188 2.2.1.2 *Functionalized MNPs*

189
190 The next few paragraphs will discuss attempts to increase the performance of MNPs by
191 functionalization of the particle surface with various chemical species in order to hone in on
192 specific affinities of the heavy metal ions and remove them from water. While such approaches
193 can improve performance, they also add cost and complexity to adsorbent preparation.

194 In order to increase efficiency and to avoid interference from other metals ions, MNPs have
195 been functionalized in order to tune their adsorption ability, creating a more effective process.⁴⁴
196 ⁵⁶ Warner *et al* engineered superparamagnetic MNPs from iron oxide via high temperature
197 deposition according to a previously published method⁵⁷ and functionalized (tuned) their surface
198 to match the affinity of specific classes of heavy metal contaminants.⁵⁶ The ligands attached to
199 the magnetite through ligand exchange reaction of lauric acid were as follows to yield
200 functionalized magnetic nanoparticle sorbents: ethylenediamine tetraacetic acid (EDTA); l-
201 glutathione (GSH); mercaptobutyric acid (MBA); a-thio-w-(propionic acid) hepta(ethylene
202 glycol) (PEG-SH); and meso-2,3-dimercaptosuccinic acid (DMSA). The functionalized
203 magnetic nanoparticles EDTA, GSH, MBA, PEG-SH, and DMSA had varying affinities for each
204 metal (refer to table 1).⁵⁶ The addition of a flexible ligand shell allowed for the incorporation of
205 a wide range of functional groups into the shell while leaving the Fe₃O₄ nanoparticle properties
206 intact.⁵⁶ The Warner group spiked Colombia River water with seven metals (Table 1), and
207 compared the results to commercial adsorbents as well as un-functionalized MNPs to measure
208 the efficiency of the modified particles.⁵⁶ The use of river water spiked with heavy metals allows

209 for a system representative of natural waters. The natural organic matter present in the river
210 water causes some interference due to adsorption to the MNPs, thus blocking the active surface
211 sites. The fact that the Warner group was able to get high binding affinity for these metals in
212 spiked river water suggests these particles may be practical for environmental applications.
213 Discussion regarding recyclability was not mentioned in this paper; however, it is conceivable
214 that the used iron oxide particles could be regenerated by removal of the adsorbed metals and
215 then reused for additional adsorption. Without such regeneration, the cost and amount of
216 nanomaterials increase. Regeneration itself may pose practical and cost barriers, especially since
217 iron oxide materials are soluble in the acidic media that would likely be used to remove the
218 adsorbed metals.

219 *Ge et al* reported novel Fe₃O₄ MNPs modified with 3-aminopropyltriethoxysilane (APS)
220 and copolymers of acrylic acid (AA) and crotonic acid (CA) as polymer shells
221 (Fe₃O₄@APS@AA-co-CA MNPs).⁴⁴ The use of a polymer shell prevented inter-particle
222 aggregation and improved dispersion stability of the nanostructures.⁴⁴

223 *Ge et al* concluded that the polymer modified MNPs successfully removed metal ions (Table
224 1) and from lab prepared aqueous solutions and that these particles were reusable.⁴⁴ They
225 performed recyclability studies using 0.1 M H⁺ and found the metal ion adsorption capacity
226 remained constant after 4 cycles.⁴⁴ The polymer coating assisted in preventing dissolution of the
227 metal oxide core under these acidic conditions. In 2005, *Hu et al* published a paper using
228 maghemite nanoparticles synthesized via a sol gel method⁵⁸ to remove Cr (VI) from wastewater
229 generated from a metal-processing plant.⁵⁹ According to the EPA, the acceptable level of
230 chromium in drinking water is no more than 0.1 mg/L.¹² The most common methods of
231 removing hexavalent chromium from wastewater effluent are chemical precipitation, reverse

232 osmosis, and electrochemical methods.⁵⁹ However, there are many disadvantages with these
233 approaches, with high cost being at the top of the list.⁵⁹ Hu *et al* utilized adsorption technologies
234 in an effort to efficiently remove Cr (VI) at low cost.⁵⁹ They used maghemite nanoparticles as
235 solid adsorbents to remove Cr (VI) ions, and then were able to regenerate the adsorbent.⁵⁹ The
236 regenerative studies were performed by controlling the pH.⁵⁹ After a suitable eluent was used for
237 desorption, 0.01 M sodium hydroxide was found to be the most effective at returning the
238 particles to their active form.⁵⁹ After six cycles, the Cr capacity of maghemite remained
239 unchanged.⁵⁹ In the case of maghemite nanoparticles, almost all of the adsorption active sites are
240 all located on the exterior of the nanoparticle's surface. Compared to a porous adsorbent, this
241 means that the adsorption of the Cr (VI) ions onto the maghemite particle site is faster due to the
242 accessibility of the external active sites.⁵⁹ Once all the active sites are occupied, equilibrium is
243 reached.⁵⁹ Hu *et al* found pH 2.5 to be the optimum conditions for Cr (VI) removal.⁵⁹ Hu *et al*
244 was able to demonstrate that the maghemite nanoparticles were successful at adsorbing Cr(VI)
245 ions however, representative wastewater samples typically have a pH 6-9.⁶⁰

246 The EPA lists mercury as a contaminant in drinking water with maximum contaminant level
247 of 2 $\mu\text{g L}^{-1}$. Long term exposures can cause kidney damage.¹² In 2014, Qi *et al* published a
248 water-soluble magnetite superparamagnetic nanoparticles (MSPNPs) in attempt to provide a fast,
249 selective adsorbent to remove mercury (Hg^{2+}) from water.⁶¹ In water, the polymeric molecules
250 act as a binder for any metal ions present; therefore, becoming a "carrier" of metal ions from
251 treated water.⁶² They synthesized these particles using an efficient polymer combined with the
252 MSPNPs to functionalize the magnetic nanoparticle as previously published.^{63, 64}

253 The effect of polymer modification on the surface of (M-MSPNPs) was tested on the
254 removal of Hg^{2+} from water. This was done using the batch method and a shaking speed of 350

255 rpm.⁶¹ Adsorption studies compared MSPNPs and M-MSPNPs at pH 7 (refer to table 1 for
256 details). Isotherm calculations were used to describe the behavior of the adsorption of Hg²⁺ to
257 the M-MSPNPs. The data fit to both Langmuir and Freundlich models although the Langmuir
258 was moderately better. The adsorption behavior described by the Langmuir model indicates the
259 formation of a monolayer complex between the coated polymer and Hg²⁺.⁶¹ Therefore, the
260 authors infer that no more complex molecules can form on the first layer.⁶¹ The effect of pH and
261 salinity were studied in order to obtain data representative to real water samples. Both did not
262 have a significant effect on the adsorption of Hg²⁺ to the M-MSPNPs. A sample collected from
263 Jinji Lake located in China, was spiked with Hg²⁺ and adsorption experiments were performed.
264 The model water sample gave insight as to the influence of coexisting ions and the potential
265 effect they had on the adsorption of Hg²⁺ to the M-MSPNPs. The adsorption interaction was due
266 to complex formation between the polymer ligand on the M-MSPNPs and Hg²⁺.⁶¹ Regenerative
267 studies were performed using 2-mercaptoethanol (a strong complexing agent) to effectively
268 remove the bound Hg²⁺ from the M-MSPNPs after treatment.⁶¹ After 3 cycles the percent
269 removal was higher than 98 %.⁶¹

270 The authors compared the removal efficiency of the M-MSPNPs to other reported studies
271 using different adsorbents to remove Hg²⁺ from water.⁶¹ M-MSPNPs were one of the most
272 efficient and quickest at removing Hg²⁺.⁶¹ This article was rich in data to show that these M-
273 MSPNPs would be applicable to solve real world heavy metal contamination.

274 In addition to the studies highlighted in this article, there have been several other articles on
275 functionalizing the surface of magnetic particles.⁶⁵⁻⁷¹

276 2.3 Hematite (α -Fe₂O₃)

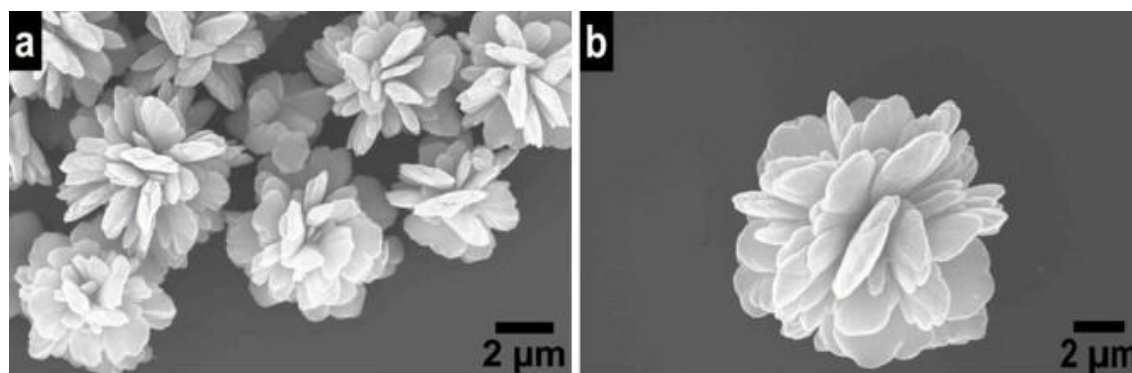
277 The use of a non-magnetic phase of iron oxide, hematite (α -Fe₂O₃), has been considered
278 as a stable, low cost material for use in sensors, catalysis and environmental applications.⁷² The
279 synthesis of iron oxide into hierarchical nanostructures with distinct shapes is of interest due to
280 their novel properties compared to bulk materials.

281 The role of nanohematite as an adsorbent for the removal of heavy metal ions from
282 spiked tap water was examined by Shipley *et al.*⁷³ This study provided a comprehensive
283 elucidation into the adsorption properties of nanohematite (α -Fe₂O₃) to certain heavy metal ions
284 in solution. Commercially bought nanohematite particles were used (refer to table one for
285 details). The parameters that were investigated included loading and exhaustion studies, the
286 effect of pH and temperature, as well as the its performance in the presence of multiple metals in
287 solution.⁷³ A representative groundwater sample was prepared by spiking treated tap water with
288 the heavy metals of interest. Batch adsorption studies were performed and the spent
289 nanohematitic particles were removed from solution via filtration. The effect of temperature on
290 the adsorption of metals to the nanohematite was carried out at pH 6 and illustrated that metal
291 adsorption increased with increasing temperature.⁷³ The effect of pH was studied to observe
292 surface charge effects on adsorption. An increase in pH correlated with an increase in metal
293 adsorption to the nanohematite. The surface chemistry was attributed to the presence of
294 hydroxyl groups located on the exterior of the nanohematite particles which allowed for specific
295 binding to the heavy metal ions.⁷³ Freundlich isotherm model was applied to describe the
296 behavior of the experimental data at all three temperatures (refer to table 1 for details). The
297 model proved that adsorption of Pb (II), Cd (II) and Cu (II) were endothermic processes and
298 Zn(II) to be exothermic.⁷³ Exhaustion studies showed that the nanohematite could be recycled
299 up to four cycles before adsorption ability was compromised. This paper provided great detail

300 into the use of nanohematite as an adsorbent for metal removal. The use of spiked tap water
301 proved that this adsorbent could be used in treatment. A similar paper was published by Grover
302 *et al* investigating the adsorption and desorption behavior of bivalent metals to hematite
303 nanoparticles.⁷⁴

304 In order to increase the surface area and efficiency of hematite, studies have been
305 published on hierarchical structures used as adsorbents to remove heavy metals from aqueous
306 solutions. Liang *et al* synthesized self-assembled 3D flower-like α -Fe₂O₃ structures for water
307 treatment use.⁷²

308 Figure 1 illustrates the α -Fe₂O₃ microflowers that were synthesized via hydrothermal
309 treatment.⁷² The size of the microflower was between 5-7 microns, however the size of each
310 “petal” was on the nanoscale, thus allowing for the enhanced surface area and properties found
311 with typical nanomaterials.⁷² These were advantageous for water treatment due to their unique
312 structural characteristics, which enables separation and regeneration.⁷²



313
314 Figure 1. SEM images of α -Fe₂O₃ microflowers after hydrothermal treatment at 150 °C for
315 12 h.⁷² Reprinted from Ref. 72, Copyright 2015, with permission from Elsevier.
316

317 The flower-like structure prevents flocculation, and the enhanced surface area with multiple
318 spaces and pores provide many active sites for interaction with pollutants.⁷² The novelty of these
319 microstructures compared to other 3D flower oxides is in the simplicity of the synthesis route. In

320 order to investigate the potential application of the α -Fe₂O₃ microflowers for water treatment,
321 adsorption isotherms were observed. Both Langmuir and Freundlich adsorption models were
322 considered (equations 1 and 2 respectively). The Langmuir model showed the best fit with
323 correlation coefficients above 0.999 when compared to the Freundlich model.⁷² Therefore it can
324 be inferred that the adsorption behavior of the heavy metal ions (Table 1) onto the α -Fe₂O₃
325 microflowers is a monolayer adsorption process.⁷² There is no mention of regenerative studies,
326 how the spent particles were removed from solution, or surface area measurements. The
327 solutions containing heavy metals were prepared in the lab and no mention of environmental
328 applicability was made. There have been other α -Fe₂O₃ microstructures synthesized for
329 wastewater treatment. Some worth mentioning were in the shape of cauliflower⁴⁷, nanosheets,⁷⁵
330 3D self-assembled iron hydroxide nanostructures⁷⁶ and nano-flowers.^{77, 78} The two former
331 studies reported the removal of dyes from wastewater and not metal ions. The latter studies with
332 the iron oxide nanoflowers reported heavy metal removal applications.

333 Other reports for the use of bulk hematite as adsorbents for heavy metal removal have
334 been published.⁷⁹⁻⁸¹ However, since the focus of this article is on inorganic nanoadsorbents for
335 heavy metal removal, these will not be discussed in great detail.

336 2.3.1.1 *Iron Oxide Scopes and Limitations*

337
338 Iron oxide limitations include poor recovery (hematite) and the size of the particle can be
339 a factor on its overall performance.³⁷ In the case of MNPs, if they are too small (< 12 nm)
340 magnetic separations would require large external magnetic fields to overcome opposing forces,
341 which can lead to costly gradient separators.^{82, 83} The research discussed above did not mention
342 the possibilities of scaling up the syntheses for the iron oxide nanomaterials in order to

343 demonstrate their real world application to remove heavy metals from wastewater effluent.

344 However, iron oxide is abundant, relatively non-toxic and cheap.

345 2.4 Carbon Nanotubes with other metals/supports

346 Carbon nanotubes are often combined with other metals or types of support in effort to
347 enhance their overall adsorption, mechanical optical, and electrical properties.

348 A study published by Di *et al*, reported the use of carbon nanotubes as a support for the rare
349 earth element cerium (Ce) in the form of cerium oxide (CeO₂).⁸⁴ The researchers reported rare
350 earth elements in the hydrous oxide form demonstrated high-adsorption capacity for anions
351 therefore by supporting ceria nanoparticles onto CNTs (CeO₂/ACNTs), they would create a
352 novel adsorbent for wastewater treatment.⁸⁴ Hydrous oxides of rare earth elements have
353 previously been found to have a high affinity for anions such as fluoride, arsenate and
354 phosphate.^{85, 86} Synthesis of the aligned carbon nanotubes (ACNTs) was achieved via previously
355 published method⁸⁷ by catalytic decomposition of hydrocarbon.⁸⁴ The ceria nanoparticles were 6
356 nm in diameter. A solution containing CeCl₃ was added in small volumes to the CNTs to make a
357 CeO₂/ACNTs support.⁸⁴ It is well known that the addition of nitric and sulfuric will add –OH
358 and –COOH functional groups to CNTs. The CeO₂/ACNTs were functionalized with the
359 aforementioned acids and the effect of pH, adsorption capacities, isotherm results and
360 comparison to other adsorbents were reported. Di *et al* found that the pH was the most important
361 parameter when considering the binding of the metal ion to the CeO₂/ACNTs.⁸⁴ They evaluated
362 adsorption pH effects from pH 3.0-7.4, pH 7 being the optimal value.⁸⁴ Adsorption studies were
363 performed at 25°C and the CeO₂/ACNTs demonstrated high Cr (VI) adsorption efficiency from
364 water with variable pH ranges (3.0-7.4).⁸⁴ Langmuir and Freundlich isotherm algorithms were
365 applied and the results showed an adsorption capacity two times higher when compared to other

366 adsorbents (refer to table 2).⁸⁴ There was no mention of recyclability or use of actual wastewater
367 samples. Also, the use of rare earth elements for environmental remediation can be costly. Other
368 reports have been published on the use of cerium oxide nanoparticles to remove heavy metal ions
369 from pure water but without the CNT support.^{88, 89,90}

370 Gupta *et al* published a study using CNTs as a support for magnetic iron oxide.⁹¹ They
371 combined the adsorption properties of CNTs with the magnetic properties of iron oxide into a
372 “composite” adsorbent to remove chromium from water.⁹¹ They studied the adsorption of
373 chromium due to its heavy use in tanneries, glass and mining industries.⁹¹ Chromium is a known
374 contaminant and health hazard. The MWCNTs were purchased commercially and purified and
375 functionalized using nitric acid. Ferric chloride hexahydrate and ferrous chloride tetrahydrates
376 were added to a suspension of MWCNTs and after 2 h, ammonium hydroxide was added to
377 precipitate the iron oxides.⁹¹ The MWCNTs/nano-iron oxide composite was then filtered and
378 dried.⁹¹ Batch experiments were performed to study the adsorption capacity of activated carbon,
379 MWCNTs and a MWCNTs/nano-iron oxide composite.⁹¹ The results from the adsorption
380 studies were compared, and the MWCNTs/nano-iron oxide composite was better at adsorbing
381 chromium when compared to the MWCNTs and the activated carbon (refer to table 2).⁹¹ The
382 iron oxide nanoparticles have surface oxygen atoms, which can provide additional adsorbing
383 sites for the chromium.⁹¹ The presence of these oxygen atoms also increases the surface charge,
384 which can contribute to electrostatic interaction with the chromium.⁹¹ Effect of pH on the
385 adsorption of chromium and the MWCNTs/nano-iron oxide composite was evaluated. At a pH
386 range of 5-6, maximum adsorption capacity was observed. Other parameters were investigated
387 (contact time, agitation time, and loading studies)⁹¹ but no isotherm models were applied and
388 regenerative studies were not mentioned. The MWCNTs/nano-iron oxide composites were not

389 tested using real world samples, however, wastewater is typically between pH 6-9⁶⁰ which
390 suggest these composites may be environmentally applicable.

391 2.4.1.1 CNTs Scopes and Limitations

392
393 Toxicity of CNTs has been a growing concern since their discovery in the early 90s.⁹²
394 Many reports have surfaced regarding health concerns^{93, 94} Alternative methods such as using
395 CNT sheets⁹⁵ have been implemented in an effort to remove heavy metals from water without
396 the serious health^{96, 97} and environmental risks.⁹⁸ The other drawbacks with using CNTs are their
397 low removal efficiency and limited selectivity.⁹⁹ Also, the sorption capacities for metal ions are
398 very low because the walls of carbon nanotubes are not reactive.⁶² However, the CNTs can be
399 easily modified by chemical treatment^{100, 101} to correct these issues. Future directions for the
400 CNTs discussed in the previous sections would be to test their performance using real world
401 samples and help with environmental remediation and cleanup. In order to do this, the synthesis
402 of these carbon nanomaterials would need to be scaled up which could become costly in some
403 cases.

404 2.5 Metal oxide nanoadsorbents

406 The use of metal oxides for treatment provides a low cost adsorption technology. Metal oxides
407 can include ferric oxides (refer to iron oxide section for in-depth discussion), titanium (Ti),^{102, 103}
408 cerium (Ce),^{88, 89} and Zinc (Zn). When produced at the nanoscale, metal oxides can have
409 increased surface area and possess favorable sorption to heavy metals.

410 2.5.1 Titanium

411
412 The ninth most abundant element in the Earth's crust is titanium.¹⁰⁴ It is cheap and its oxide
413 is chemically inert. Titanium dioxide (TiO₂) has many applications. It has been used over a wide

414 range of applications from photovoltaics, photocatalysis, H₂ sensing, lithium batteries and as an
415 adsorbent for the removal of contaminants in polluted waters.¹⁰⁴ It's also used extensively as a
416 pigment in paints, food, pharmaceuticals and cosmetics. In addition to titanium dioxide, titanates
417 have also been used as adsorbents. Layered titanates can be formed into sheets,¹⁰⁵ fibers,¹⁰⁶
418 hierarchical shapes such as flowers,^{107, 108} and composites.^{109, 110} These shapes contribute to
419 increased surface area and higher ion exchange capabilities.¹⁰⁷ The difference between the two is
420 that titanate works through an ion exchange process.

421 2.5.1.1 *TiO₂ and Titanate*

422
423 Arsenic removal and recovery is a huge concern and challenge. Arsenic is introduced into
424 the environment via wastewater effluent from industries and in many parts of the world in
425 groundwater which poses a threat to people who drink unpurified well water. Luo *et al*
426 performed extensive work on the removal and recovery of arsenic using TiO₂.¹¹¹ They acquired
427 wastewater from a copper smelting company that contained an average concentration of 3310
428 mg/L As (III), 24 mg/L Cu, 5 mg/L Pb, and 369 mg/L Cd.¹¹¹ The pH of the solution was 1.4 but
429 was adjusted to 7 for the adsorption batch experiments. Titanium dioxide was synthesized by
430 hydrolysis of titanylsulfate at 4°C.¹¹¹ The authors made no mention of the size of the TiO₂ and
431 did not provide images. Surface area was measured and is reported in table 3. Regenerative
432 studies were investigated. The spent TiO₂ was collected through membrane filtration, and then
433 the “filter cake” was mixed with a basic solution. The solid was collected and reused in the
434 batch adsorption method. Luo *et al* reported 21 successive treatment cycles using the
435 regenerated TiO₂. Arsenic was recovered by pre-concentrating the extracted solutions (TiO₂
436 included), and further precipitated as a result of cooling.¹¹¹ Adsorption kinetic experiments were
437 performed using batch method. Results were fit with a pseudo second-order kinetic model with

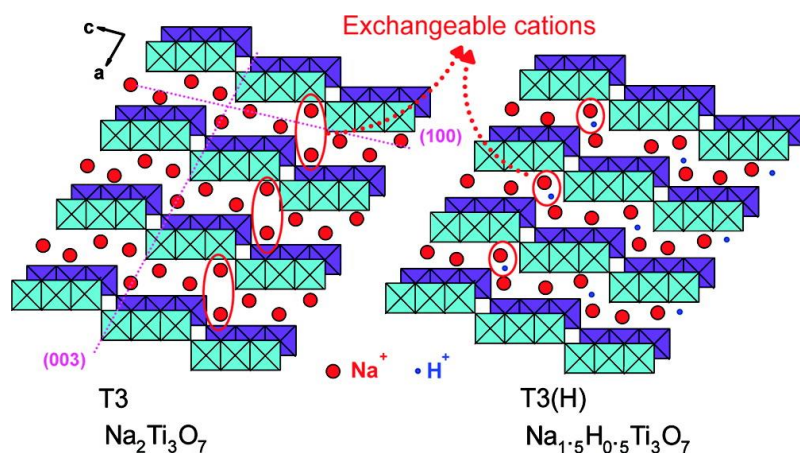
438 an R value greater than 0.999 and a rate constant of 0.84 g/mg-h. A majority of the arsenite was
439 adsorbed in less than one hour reach about 100 mg/g which was steady state and remained there
440 for 25 hours, the initial concentration was 3310 mg/L.¹¹¹ Since As (III) forms “inner-sphere
441 bidentate binuclear complexes”,¹¹² it will bind to the OH surface sites on the TiO₂.¹¹¹ This result
442 was confirmed using Extended X-ray Absorption Fine Structure spectroscopy (EXAFS), XPS
443 and surface complexation modeling. Attempts to implement this technique to full scale were
444 limited. The authors state that the TiO₂ used in this study was expensive in comparison to the
445 process that was currently in place to remove arsenic at the copper smelting plant (metal
446 hydroxide process).¹¹¹ Nonetheless, this paper provided extensive work on the removal and
447 recovery of arsenic from real world samples. Furthermore, TiO₂ exhibited great regenerative
448 studies which may reduce the overall cost in the future for the copper smelting plant.¹¹¹

449 Engates and Shipley studied the adsorption of metal ions (refer to table 3) to commercial
450 TiO₂ nanoparticles and TiO₂ anatase bulk particles.¹¹³ San Antonio tap water was spiked with
451 heavy metals in effort to have a model polluted water sample.¹¹³ Adsorption studies were carried
452 out for single and multi-metal adsorption. Exhaustion experiments were also performed. The
453 authors reported large adsorption capacities for the TiO₂ nanoparticles compared to bulk
454 particles.¹¹³ The data correlated to Langmuir isotherm model indicating a monolayer adsorption
455 on the surface of the TiO₂ nanoparticles. The TiO₂ nanoparticles also exhibited strong
456 adsorption rates when compared to the bulk particles. Exhaustion results showed that at pH 6,
457 TiO₂ nanoparticles exhausted after 3 cycles and at pH 8 after 8 cycles.¹¹³ These results support
458 the possibility of TiO₂ nanoparticles to be a potential remediation for heavy metal removal from
459 contaminated waters. Other reports by this group studied regeneration of TiO₂ nanoparticles for
460 heavy metal removal.¹¹⁴

461 Layered protonated titanates have become the latest sensation in solar cells, lithium ion
462 batteries, and as adsorbents.^{104, 105} According to Lin *et al*, “unfolded” titanate nanosheets have a
463 high theoretical cation exchange capacity due to the presence of exchangeable cations
464 intercalated in the interlayers.^{104, 105} This ability makes them good adsorbents through ion
465 exchange. Layered protonated titanate nanosheets (LPTN) were produced using a one-pot
466 synthesis of titanium n-butoxide with urea at low temperatures. The urea was added to govern
467 the production of NH_4^+ ions into the TiO_6 layers.¹⁰⁵ Extensive characterization of different
468 crystal phases and structures were investigated. Sample number “400-7” was found to be the
469 best model adsorbent for this study. Adsorption studies using Pb^{2+} as the model pollutant and an
470 organic dye, methylene blue with the LPTN were conducted. Results are reported in table 3.
471 Isotherm models were applied, Langmuir describing the best fit for the data. Favorable
472 adsorption was observed for Pb^{2+} with the LPTN. The authors state the mechanism of adsorption
473 for the Pb^{2+} onto the LPTN was due to the negative zeta potential of the LPTNs in water.¹⁰⁵ This
474 negative potential created an electrostatic bond between the cationic Pb^{2+} and the surface of the
475 negative LPTN.^{105, 115} Furthermore, the Pb^{2+} ions were intercalated into the interlayers of the
476 LPTNs, thus making it a successful adsorbent for Pb^{2+} removal from water.¹⁰⁵ No natural water
477 samples were used for this study so it is unclear whether other metals or ions could interfere with
478 the intercalation of Pb^{2+} ions in the LPTN interlayers. However, the LPTN shows promise for
479 industrial applicability for its ability to remove inorganic and organic contaminants (methylene
480 blue) from water.

481 Additional structures of layered titanates have been used as adsorbents to remove heavy
482 metals from solution. Titanate nanofibers were synthesized by Yang *et al* to remove radioactive
483 contaminants and metals from contaminated water. The fibers were synthesized under

484 hydrothermal conditions and consisted of two TiO_6 octahedra connected to form layers (figure 2
 485 below).^{106, 116, 117}



486

487 Figure 2. Schematic of the nanofiber structures.¹⁰⁶ Reprinted with permission from Yang *et al.*
 488 Copyright 2015 American Chemical Society.

489

490 The layers have the ability to carry negative electrical charges and contain exchangeable sodium

491 cations.¹⁰⁶ The titanate nanofibers were synthesized via hydrothermal treatment and then

492 subsequently dried into a white powder. The white powder product was collected and labeled

493 “T3”. Excess “T3” was then dried a second time at 483 K to obtain “T3(H)”.¹⁰⁶ The T3 phase

494 was $\text{Na}_2\text{Ti}_6\text{O}_{13}$ and the T3(H) phase was $\text{Na}_{1.5}\text{H}_{0.5}\text{Ti}_3\text{O}_7$.¹⁰⁶ The authors hypothesized that the

495 mechanism of sorption of the pollutant cations onto the fibers was due to the induction of

496 structural changes that permanently trap them inside the layers of the adsorbent.¹⁰⁶ To test the

497 adsorption performance of the T3 and T3(H) titanate nanofibers, isotherm and sorption studies

498 were investigated (refer to table 3).¹⁰⁶ In brief, Yang *et al* found that the T3(H) fibers were better

499 at selectively binding to the Pb^{2+} and radioactive ions than the T3 fibers.¹⁰⁶ In order to be an

500 effective adsorbent for radioactive elements, the titanate nanofibers had to permanently trap the

501 radioactive cations and Pb^{2+} for safe disposal.¹⁰⁶ The release of these cations was investigated

502 via centrifugation and basic treatment. No release of the Pb^{2+} ions was observed. The authors

503 concluded that the fibers were trapping the ions and could be stored without causing secondary

504 contamination.¹⁰⁶ Large-scale synthesis and industrial use of the titanate nanofibers was
505 discussed but not applied.

506 The last two sections discussed the use of sheets and fibers as inorganic nanoadsorbents
507 for heavy metal removal. Other groups have taken these titanate structures a step further and
508 have prepared hierarchical titanate structures, titanate nanoflowers (TNF), in an effort to improve
509 the overall surface area.¹⁰⁷

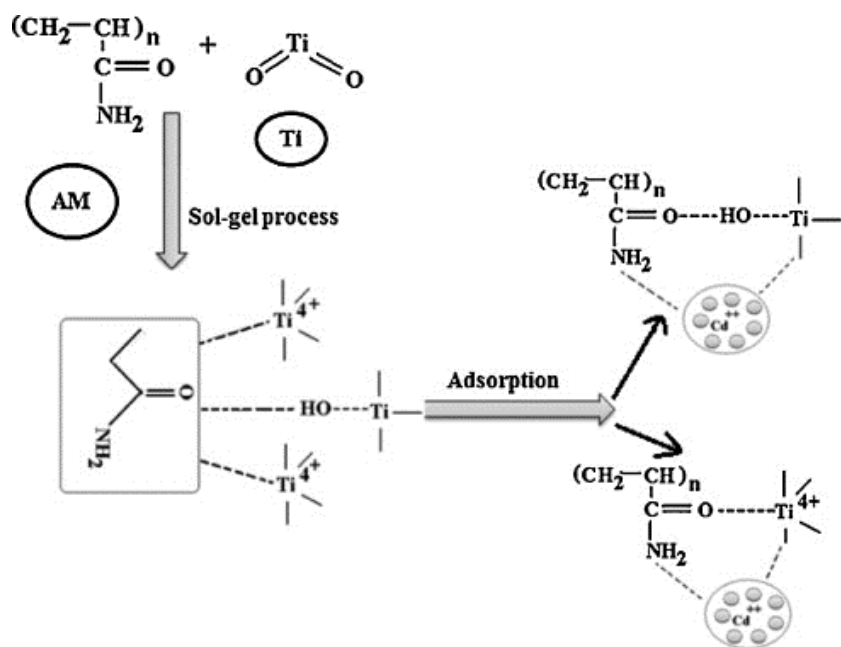
510 Huang *et al* reported a study using TNF to remove heavy metal ions from wastewater (refer to
511 table 3 for details). The idea behind using the TNF vs. TNT or TNW is the titanate flowers have
512 ultra-thin nanosheets which can prevent aggregation, and provide strong mechanical properties
513 when applied in water flow systems.¹⁰⁷ The TNF, TNT and TNW were all synthesized using an
514 alkaline hydrothermal method and further acidified to convert them into a protonated form.¹⁰⁷

515 To get each form, the synthesis time for TNF was 45 minutes, TNT was 2 h and TNW was 6
516 h.¹⁰⁷ The authors believed that the TNF was an intermediate product of the TNT since it is a
517 flowerlike aggregate of many sheets.¹⁰⁷ Competitive adsorption studies using TNF, TNT, and
518 TNW were performed using a ternary system containing Zn (II) Ni (II) and Cd (II). TNF
519 adsorbed to all three of the cations better than TNT and TNW.¹⁰⁷ Adsorption isotherms were
520 studied and compared among the titanate nanostructures. The TNF showed the largest adsorption
521 capacity when compared to the TNT and TNW which was about 1.5×10^{-3} mol/g Pb(II) compared
522 to 6×10^{-4} mol/g Pb(II) for TNW and 4×10^{-4} mol/g Pb(II) for TNT. Adsorption kinetics for the
523 titanate nanostructures was considered in effort to design a treatment plan for practical
524 environmental application. The TNF exhibited the fastest adsorption for Pb (II) compared to
525 TNT and TNW (refer to table 3 for actual values).¹⁰⁷ The authors argue that the ultra-thin
526 nanosheets are able to transport heavy metal ions through the space in-between the nanosheets

527 making a “tunnel”.¹⁰⁷ The tunnels increase the diffusion rate of the Pb (II) ions and the thin
528 width of the nanosheet allows for quick access from the surface active sites to the interlayer of
529 the titanate.^{107, 118} The use of titanate nanoflowers as adsorbents for heavy metals in a model
530 pollutant system showed great promise. It would be interesting to see how the TNF would
531 perform in a real wastewater sample. There was no mention of the effect of pH in this study;
532 however, the authors did mention that the synthesis is simple and feasible for scale up
533 considerations.¹⁰⁷

534 2.5.1.2 *TiO₂ supports/composites*

535
536 In order to create a synergistic effect, TiO₂ and titanate can be combined with other
537 materials as a support or composite to enhance their properties. Cadmium is a toxic heavy metal
538 that can cause harmful health issues (hypertension, cancer, bone sores). It is introduced into the
539 environment through mining, smelting, and alloy manufacturing.¹¹⁰ Sharma *et al* developed a
540 titanium nanocomposite (TiO₂-AM) by in situ doping acrylamide (AM) into titanium during a
541 sol-gel reaction¹¹⁹ in order to develop a low cost adsorbent for cadmium removal.¹¹⁰ The
542 addition of the acrylamide to the TiO₂ forms a composite with free amide groups, which can
543 increase the binding capacity of titanium to other metals.¹¹⁰ Figure 3 illustrates the proposed
544 mechanism of adsorption. The TiO₂-AM performance as an adsorbent for Cd (II) was
545 demonstrated through sorption kinetics. Initially, the removal of Cd (II) was fast and more than
546 50 % was adsorbed in 30 minutes then reached equilibrium at 1.5 h.¹¹⁰ The authors report that
547 the initial fast rate of Cd (II) removal was due to the many unoccupied sites in the TiO₂-AM
548 composite and the adsorption was due to a “chemisorption phenomenon”.¹¹⁰



549

550 Figure 3. Proposed structure of the nanocomposite synthesis and reaction pathways for the
 551 adsorption of Cd(II) by the nanocomposite.¹¹⁰ Reprinted from Ref. 110, Copyright 2015, with
 552 permission from Elsevier.
 553

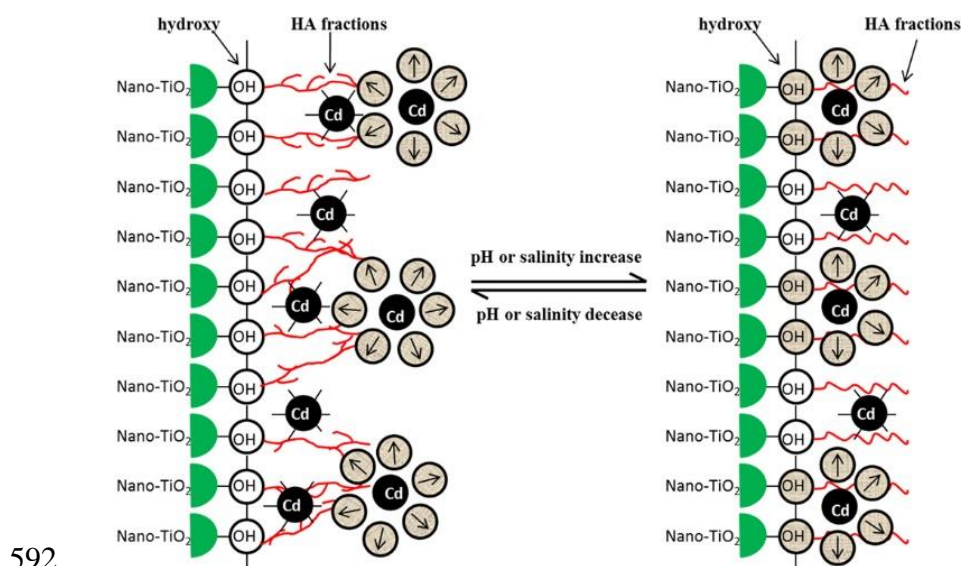
554 The effect of pH was considered at a range from 2.0-10 with pH 8 being the optimum value for
 555 Cd (II) adsorption.¹¹⁰ Sharma *et al* mentioned that Cd is very sensitive to changes in the pH due
 556 to the polar interaction of the charged Cd^{2+} species and the oxygen on the TiO_2 .¹¹⁰ Since
 557 wastewater is composed of many different types of cations and anions, the TiO_2 -AM
 558 nanocomposite was placed in separate solutions containing anions (Cl^- , $(\text{SO}_4)^{2-}$ and $(\text{CO}_3)^{2-}$) and
 559 cations (Pb^{2+} , Cu^{2+} , Co^{2+} , Zn^{2+}) with cadmium.¹¹⁰ These ions interfere with the binding to the
 560 TiO_2 -AM nanocomposite and have a negative impact on adsorption as well as forming
 561 complexes with the cadmium making it challenging to remove from the wastewater.¹¹⁰ The
 562 increasing concentration of the anions decreased the adsorption capacity for the cadmium.¹¹⁰
 563 The cations showed an interference of less than 10 % which is not significant for Cd (II)
 564 removal.¹¹⁰ Adsorption isotherms were studied and the Cd (II) data best fit to the Langmuir
 565 model.¹¹⁰ This is indicative of monolayer adsorption capacity. In order to test the regenerative

566 ability of the TiO₂-AM nanocomposite, desorption studies were performed. After the fifth cycle,
567 the authors observed a decrease in the adsorption efficiency and desorption efficiency. The
568 synthesis of TiO₂-AM nanocomposite did require a lot of time and the temperature for adsorption
569 was a little higher than room temperature. However, the fact that it can be regenerated through
570 five cycles does show promise as a scale up adsorbent for industrial applications. The TiO₂-AM
571 nanocomposite was not used in natural water systems; however, the extensive research
572 investigating its performance in the presence of interference ions gave promising results. Other
573 studies were reported for titania composites. Byrne *et al* published a paper on mercury removal
574 by adsorption and photocatalysis using silica-titania composites (STCs).¹⁰⁹ Without illumination
575 (adsorption only), the STCs removed 90 % of mercury when compared to unmodified TiO₂
576 (Degussa P25). The combination of photocatalysis and adsorption to simultaneously remove
577 organic pollutants from aqueous solution is an innovative technology that has potential for
578 environmental applications. The pH value of these systems was lower than actual reports of pH
579 values for wastewater (pH 6-9).⁶⁰ No natural water samples were used in this study.

580 2.5.1.3 TiO₂ coatings

581
582 Generally, coating the surface of TiO₂ nanoparticles is a method used to increase
583 adsorption and improve technology for removal of heavy metals in aqueous solution. As
584 discussed previously, humic acid (HA) is a form of natural organic matter (NOM) found in the
585 aquatic environment. It is known that NOM plays an important role in the sorption of heavy
586 metals and other toxic pollutants.¹²⁰ Coating with HA applies a polyanionic coating onto metal
587 oxides, which can change the surface chemistry properties.¹²¹ Chen *et al* coated humic acid onto
588 TiO₂ through mechanical agitation from a previously published method.^{120, 121} Figure 4 shows
589 the effect of HA interactions on HA-TiO₂ when the solution conditions were changed. However,

590 the main purpose for the inclusion of figure 4 was to show the proposed structure and coating of
 591 the HA on to nano-TiO₂.¹²¹



593 Figure 4. Effect of HA fractions on HA-TiO₂ during different solution conditions.¹²¹ Reprinted
 594 from Ref. 121, Copyright 2015, with permission from Elsevier.

595 Coating nano-TiO₂ with HA added phenolic groups to the surface and interacted with terminal
 596 OH groups on the surface of the nano-TiO₂.¹²¹ The authors chose Cd (II) as a model pollutant
 597 and studied the effect of pH, role of salinity and performed adsorption experiments. Overall, the
 598 results showed that HA-TiO₂ increased adsorption to Cd (II) compared to nano-TiO₂. It was
 599 suggested that this was due to the fact that the presence of HA modifies the bioavailability of
 600 heavy metals in aquatic systems.¹²¹ Both salinity and pH changed adsorption interactions of Cd
 601 (II) to the nanoparticles. High pH and salinity contributed to electrostatic attraction between the
 602 charges on the particle. Low salinity facilitated covalent bond interactions.¹²¹ The HA-TiO₂
 603 showed a moderate increase in adsorption when compared to the nano-TiO₂ (refer to table 3).
 604 Adsorption isotherms were calculated and the Freundlich model showed the best fit.¹²¹ Overall,
 605 this study provided insight as to how HA and nano-TiO₂ interacted with heavy metals in a
 606 representative environmental sample. It would be interesting to observe the interactions of HA-

608 TiO₂ with binary and ternary solutions containing other heavy metals. Regenerative studies were
609 not performed.

610 2.5.1.4 Titanium Scopes and Limitations

611
612 Limitations of TiO₂ for applications in water treatment is mainly due to its small particle
613 size which can lead to expensive filtering treatment.¹²² However, much progress has been made
614 to address this issue using innovative nanocomposites containing TiO₂ or titanate with polymers,
615 metals and humic acid¹²¹ as previously discussed. The hydrothermal methods for TiO₂
616 nanomaterials seem to be the most economical when it comes to scaling up the reactions for
617 water treatment. Another concern is the emerging studies reporting on the toxicity of TiO₂ based
618 nanomaterials.¹²³⁻¹²⁵

619 2.5.2 ZnO nanoparticles

620 There is limited literature on the use of zinc oxide as an adsorbent to remove heavy
621 metals in solution. Typically, its used to treat H₂S contamination.¹²⁶ Nonetheless, it is widely
622 popular for use in other technologies such as gas sensing, photocatalysis and solar cells.¹²⁷ It is
623 considered nontoxic to the environment. The many surface hydroxyl groups make it a promising
624 candidate for heavy metal adsorption in aquatic systems.

625 ZnO nanoparticles were used as an adsorbent to remove Zn(II), Cd (II) and Hg (II) ions
626 from aqueous solutions in a study reported by Sheela *et al.*¹²⁸ The ZnO nanoparticles were
627 synthesized using the precipitate method then dried and calcined at 400°C.¹²⁸ The batch method
628 was employed to measure the adsorption of the heavy metal ions onto ZnO nanoparticles. The
629 metal ions adsorbed onto the ZnO at different concentrations, however, Hg (II) had the highest
630 maximum adsorption (refer to table 3 for details). The authors state that this was because Hg (II)
631 has the smallest hydrated ionic radii (compared to Zn and Cd), which allowed it to move faster in

632 solution and reach the adsorption sites on the ZnO particle.¹²⁸ Also, Hg has a higher
633 electronegativity value when compared to the other cations. The effect of pH and temperature on
634 adsorption was studied with the maximum value at 5.5 and 30°C respectively.¹²⁸ Isotherm
635 models were applied and the adsorption data fit well to both Langmuir and Freundlich. The
636 mechanism for sorption between the cations and ZnO nanoparticles could be due to both ion
637 exchange and adsorption processes.¹²⁸ The authors infer that if ion exchange process is
638 occurring then the ions must be moving either through the channels within the crystal lattice or
639 the pores of ZnO mass.¹²⁸ Previous studies have reported on metal ions replacing cations with
640 surface hydroxyl groups.¹²⁹ The experimental data collected from the pH studies supported this
641 finding. Further work was done looking at adsorption kinetics, contact time and
642 thermodynamics. Natural water samples were not used in this study and no regenerative
643 experiments were considered. Published work by Salehi *et al* engineered Chitosan-zinc oxide
644 nanoparticles for dye removal with potential to remove other pollutants.¹³⁰

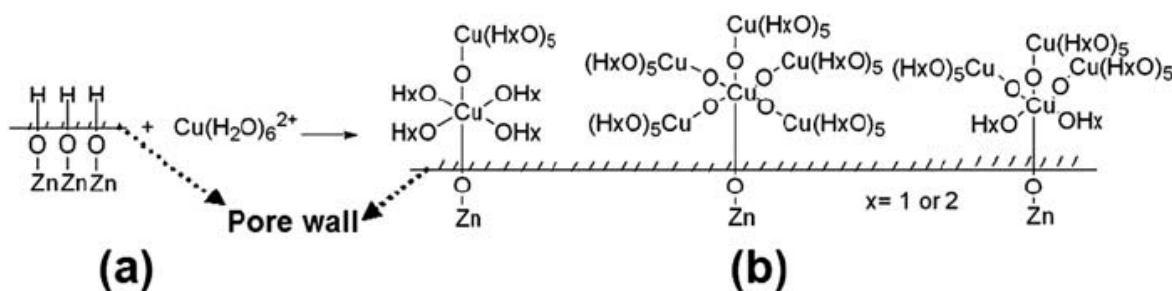
645 In order to improve the adsorption efficiency of ZnO, Wang *et al* fabricated hollow ZnO
646 hollow microspheres using a previously published hydrothermal method.^{131, 127} They compared
647 the adsorption performances of commercial ZnO nanopowder, ZnO nanoplates¹³² and activated
648 carbon with the ZnO hollow spheres (table 3). Adsorption studies were carried out using the
649 batch method. In every case, the ZnO hollow microspheres had the highest adsorption
650 performance. Furthermore, no saturation was observed with Cu (II) concentrations higher than
651 2000 mg/L. This high adsorption value was close to the ZnO nanoplates (surface area 147
652 m²/g)¹³² however, the ZnO hollow microspheres have much less specific surface area 46 m²/g.¹²⁷
653 Previous literature along with XPS and DRIFT measurements, confirm that hydroxyl groups on
654 the surface of the ZnO hollow microspheres are interacting with the cation species forming Cu-

655 O, Pb-O or Cd-O by Lewis interactions.¹³³ Langmuir and Freundlich Isotherm models were
656 applied to study the behavior of each adsorbent. The commercial ZnO fit to Langmuir isotherm
657 model suggesting monolayer adsorption. The ZnO hollow microspheres fit to both Langmuir
658 and Freundlich models, indicating monolayer adsorption and multilayer adsorption. The authors
659 explain that the structure of the ZnO hollow microspheres plays an important role in the
660 adsorption behavior.¹²⁷ The ZnO nanosheets are cross-linked in the porous hollow spheres
661 creating non-polar and polar surfaces. Depending on the electronegativity of the metal, either the
662 Langmuir or Freundlich behaviors will predominate. For example, metals with low
663 electronegativity will fit well with Langmuir-type adsorption behaviors. There was no report of
664 the regenerative ability for the ZnO hollow microspheres. Also, they would be unstable in strong
665 acid or alkali solutions.¹²⁷ The environmental applicability of the ZnO hollow microspheres is
666 unknown due to the lack of research using natural water samples.

667 2.5.3 ZnO nanoplates and nanosheets

668 Wang *et al* synthesized micro/nanostructured porous ZnO nanoplates for use as an adsorbent for
669 heavy metal removal.¹³² They were synthesized via solvothermal methods using ethylene glycol
670 to control the morphology and subsequent annealing. The ZnO nanoplates are porous with two
671 terminal non-polar planes.¹³² The authors realized the ethylene glycol (EG) played a roles in the
672 morphology of the ZnO nanoproducts.¹³² The more EG they added, the more changes in
673 morphology was observed.¹³² The nanosheets evolved into plates, particles and finally
674 microspheres. Adsorption studies were performed with Cu (II) ions as the model pollutant. ZnO
675 nanoplates were compared to commercial ZnO nanopowder (table 3). A noteworthy mention is
676 that the adsorption behaviors for each ZnO nanomaterial were different. The ZnO nanoplate was
677 best described using the Freundlich model which indicates that the adsorption occurs on a
678

679 heterogeneous surface.¹³² Whereas the ZnO nanopowder was best fit to the Langmuir model,
 680 suggesting monolayer adsorption onto a uniform surface.¹³² The mechanism for adsorption of
 681 Cu(II) ions onto the ZnO nanoplates was due to their structure and many pores.¹³² In theory, the
 682 pore walls should contain many polar sites within the plates. Once the plates are subjected to air
 683 and water, hydroxyl radical groups should form on the sites. These results were confirmed by
 684 FTIR. In reference to the Cu (II) interaction with the ZnO nanoplates, the Cu (II) can react with
 685 the hydroxyl groups through Lewis interactions.¹³² The authors also state that the adsorbed
 686 hydrated Cu (II) ions can form Cu-OH through hydrolysis and further form Cu-O-Cu on the
 687 walls of the pores.¹³² This confirms the behavior of Freundlich because multilayer adsorption is
 688 occurring. This phenomenon is shown in an illustration provided by the author (Figure 5
 689 below).¹³²



690
 691 Figure 5. An adsorptive illustration of Cu(II) ions on the polar sites of pore walls within the
 692 porous ZnO nanoplates.¹³² Reproduced from Ref. 132 with permission from The Royal Society
 693 of Chemistry.
 694

695 Chromate anions and methyl orange were selected to investigate the possibility of anionic
 696 interference.¹³² No adsorption of these anions was observed for the ZnO nanoplates. The
 697 authors comment that further work is needed to study regenerative life. No studies were
 698 conducted to study the performance of the ZnO nanoplates in wastewater.

699 An article published by Ma *et al* used ZnO nanosheets for Pb²⁺ removal. ZnO nanosheets
700 were synthesized using a hydrothermal method with zinc nitrate and thiourea in water.¹³⁴ Their
701 objective was to use the ZnO nanosheets as an adsorbent while simultaneously doping them with
702 Pb²⁺ and use the properties of the Pb²⁺ to then create a secondary nano-adsorbent, in this case
703 ZnO/PbS heterostructured nanocomposite.¹³⁴ The ZnO/PbS nanocomposite would then have
704 wide range of functionalities including photocatalysis.¹³⁴

705 Adsorption studies were implemented using the batch method. After adsorption, the ZnO
706 nanosheets with the adsorbed Pb²⁺ were treated hydrothermally as previously mentioned. The
707 mechanism of adsorption for the Pb²⁺ onto the ZnO nanosheets was due to the hydroxyl groups
708 on their surface.¹³⁴ The metal ions in solution reacted with the hydroxyl groups, which was
709 demonstrated by the high removal capacity. Once the Pb²⁺ adsorbed to the surface of the ZnO
710 nanosheets, the products formed were PbO₂ or PbS.¹³⁴ Both of which have good photoelectric
711 abilities. The effect of pH was not considered during the adsorption studies. However, the
712 objective of this study was focused on creating a functional ZnO/PbS nanocomposite.¹³⁴ Future
713 studies should consider heavy metal removal from actual water and wastewater samples using
714 these nanocomposites. Other studies have reported the use of ZnO nanosheets for cadmium
715 removal.¹³⁵

716 2.5.4 ZnO Scopes and Limitations

717
718 There is limited literature on the use of ZnO as an adsorbent to remove pollutants from
719 aqueous solutions. Other studies have used ZnO to load onto supports in effort to create a hybrid
720 adsorbent. Kikuchi *et al* published an extensive analysis on the effect of ZnO loading onto
721 activated carbon.¹³⁶ There have been reports of coating the surface of ZnO with humic acid to
722 remove phenanthrene but no mention of its applicability for heavy metal removal was made.¹²⁰

723 Other studies have reported on the use of semiconductor nanocrystals, notably, ZnS. Amiri *et al*
724 published work on the development of CdS/ZnS core-shell nanoparticles for heavy metal
725 removal from aqueous solutions.^{137, 138} Zan *et al* used ZnS nanocrystals for Hg(II) removal.
726 These studies will not be mentioned further because the focus of this discussion is dedicated to
727 the use of ZnO nanomaterials.

728 2.5.5 *Metal Oxides Scopes and Limitations*

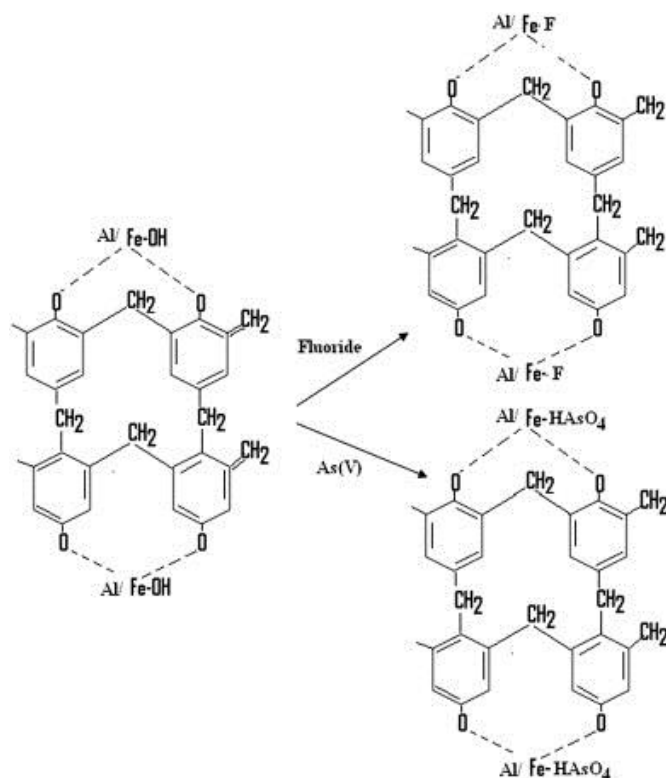
729
730 There are a few limitations to using nanosized metal oxides as adsorbents. Reducing metal
731 oxides to nanoscale sizes can increase surface area, but this increase can also cause instability.¹³⁹
732 As a result of being unstable, they become more prone to agglomeration due to the presence of
733 van Der Waals forces and other interactions.¹⁴⁰ Once these interactions occur, they lose high
734 capacity, selectivity and develop poor mechanical strength. To circumvent these limitations,
735 metal oxides are typically incorporated into supports or other bulk adsorbents.¹³⁹

736 737 2.6 Polymeric Nanoparticles

738 Polymeric nanoparticles were developed in the 1960s for use in gel permeation
739 chromatography.¹⁴¹ These adsorbents are typically made up of polystyrene or polyacrylic ester
740 matrix. They are currently used in the removal of organic pollutants from natural and
741 wastewaters. They possess physical properties including large surface area, perfect mechanical
742 rigidity, tunable surface chemistry and pore size distribution and are reasonably regenerative.¹⁴⁰
743 These novel properties allow polymeric nanoparticles to be applied for use in drug delivery,¹⁴²
744 optics,¹⁴³ and water treatment.⁶² They can also be incorporated with other particles making them
745 extremely versatile. This section will be devoted to the practical application of polymeric
746 nanoparticles for the removal of heavy metals ions for water treatment.

747 The use of polymer-based inorganic hybrid adsorbents was an alternative to try and
748 overcome the limitations of the use of metal hydroxides as adsorbents namely, issues with mass
749 transport and pressure drops using flow systems.¹⁴⁰ The solution was to impregnate or coat the
750 particles with polymers (refer to functionalized MNPs section 2.2.1.2) or fabricate a hybrid
751 adsorbent in a polymer matrix.¹⁴⁰ Kumar *et al* developed a bi-metal doped micro and nano
752 multi-functional polymeric adsorbent to remove fluoride and arsenic (V) from wastewater.²⁵
753 They synthesized polymeric beads through suspension polymerization and incorporated Al and
754 Fe salts during the polymerization step.²⁵ Briefly, the prepared polymeric beads were then
755 carbonized and activated in a tube furnace. Four different adsorbents were synthesized using
756 different metal loadings and were labeled as APH-04 (4g Fe salts), APH-22 (2g Al and Fe salts),
757 APH-40 (4 g Al salts) and PH22BM-A (APH-22 beads that were crushed by ball milling to 200
758 nm).²⁵ Adsorption experiments were performed using batch method with solution of arsenic and
759 fluoride (refer to table 4 for details). The Fe-doped micro sized beads had a larger As capacity
760 than the Al-doped beads and the Al-doped beads had a larger fluoride capacity than the Fe-doped
761 beads.²⁵ Overall, the PH22BM-A nanoparticles showed the highest adsorption capacity for the
762 As and fluoride.

763 The authors' state that the large surface area combined with the large number of active sites
764 available was the reason for its superior adsorption performance.²⁵ The surface interactions and
765 proposed mechanism of the metal doped polymeric beads after As and fluoride adsorption is
766 described in figure 6. Langmuir and Freundlich isotherm models were studied to describe the
767 adsorption behavior of the adsorbents. The Freundlich isotherm correlated with the data better
768 than the Langmuir model suggesting multilayer adsorption with heterogeneous surface
769 energies.²⁵



770

771 Figure 6. The postulated molecular structure of phenolic polymeric beads after the adsorption of
 772 fluoride and As(V) ions.²⁵ Reprinted from Ref. 25, Copyright 2015, with permission from
 773 Elsevier.

774

775 The effect of pH was studied and the maximum variation of pH observed with PH22-BM-A was

776 around 0.7 therefore a suitable pH range was between 6.0-7.5.²⁵ No real world samples were

777 used in this study. The authors mentioned a limitation of using PH22-BM-A in a flow method for

778 wastewater treatment would require a binder phase to prevent entrainment of the nanoparticles.²⁵

779 Regenerative studies were being considered in future research.

780 2.6.1.1 Polymeric Scopes and Limitations

781

782 The last section covered the use of polymeric adsorbents and how they have been used as

783 adsorbents for heavy metal removal in water. The drawbacks of this adsorbent include synthesis

784 challenges and the difficulty of implementing into environmental application. Pan *et al* stated

785 that even though polymeric adsorbents have excellent properties, for example structure, pore

786 sizes and tunable functional groups, the molecular design still has some flaws.¹⁴⁰ The ability to
787 make it highly selective for a given pollutant is a challenge and recovery can be costly if a low
788 purity polymer is used.¹⁴⁰ It is also noted that the adsorption capacities of polymeric adsorbents
789 are low and regeneration is required in order to reuse them resulting in high occupational
790 costs.¹⁴⁰

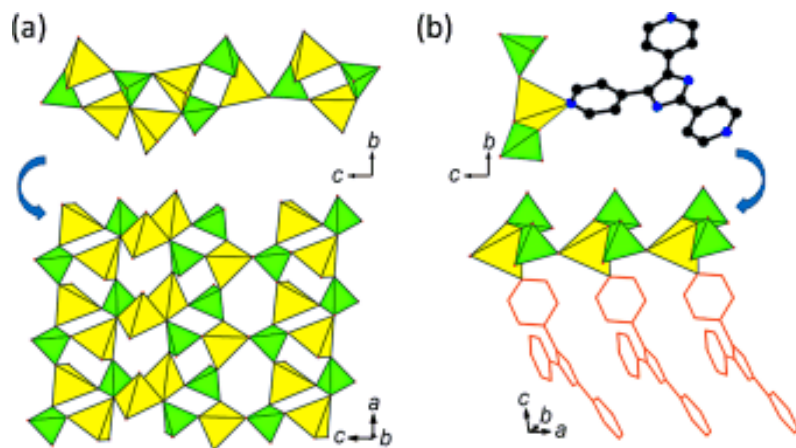
791 **3 Next Generation**

792

793 3.1 Organic-Inorganic hybrids

794 The last three sections discussed the design and use of inorganic nanoadsorbents for heavy
795 metal removal in water in extensive detail. Qi *et al* states that the next generation adsorbents for
796 heavy metal removal are organic-inorganic hybrids due to their “unique quality of combining the
797 functionality of organic compounds with the stability of inorganic compounds”.¹⁴⁴ According to
798 Wang *et al*, inorganic frameworks have various geometries, flexible coordination behaviors and
799 assorted connectivity’s which inhibit the presence of large structural pores and channels.^{145 146,}
800 ¹⁴⁷ On the other hand, metal organic frameworks possess rich structural chemistry and integrity
801 as well as potential applications in catalysis, ion-exchange, and gas storage.¹⁴⁵⁻¹⁴⁷

802 A report on the fabrication of a new organic-inorganic hybrid zinc phosphate with 28 ring
803 channels was published for the use of heavy metal removal from water. The use of organic
804 amine ligands enables a route for the synthesis of large channels into an inorganic framework.
805 The synthesis of these organic-inorganic hybrids (NCU-1) took about 2 days using
806 hydro(solvo)thermal reactions.¹⁴⁵ Figure 7 shows a proposed illustration of the NCU-1 structure.
807 For applicability for heavy metal removal, NCU-1 was added to aqueous solutions containing
808 Co, Hg, and Cd (refer to table 5 for more details).



809

810 Figure 7. Two types of chains in NCU-1: a) the inorganic $\infty[\text{Zn}_4(\text{HPO}_4)_2(\text{PO}_4)]^+$ chain with
 811 three-, four-, and six-membered rings; b) the organic-inorganic hybrid $\infty[\text{Zn}(\text{H}_2\text{L})(\text{HPO}_4)(\text{PO}_4)]^-$
 812 chain. Blue and black circles represent N and C atoms, respectively. The H atoms are omitted for
 813 clarity.¹⁴⁵ Reprinted from Ref. 145, Copyright 2015, with permission from John Wiley and Sons.

814

815 The adsorbent was removed from the water via centrifugation. The NCU-1 was capable of

816 removing metal ions from solutions however, the percentages were quite low (table 5).¹⁴⁵ The

817 authors contribute the non-coordinating N atoms of the 2,4,5-tri(4-pyridyl)-imidazole in the wall

818 of NCU-1 for the interaction with incoming metal ions.¹⁴⁵ The NCU-1 organic-inorganic hybrid

819 showed promise for environmental applicability but more research is needed to assess its

820 potential.

821 In order for organic-inorganic hybrids to be used in large-scale water remediation plants,

822 Arkas *et al* states the technique has to be low cost, marginally non-toxic in reference to the types

823 of chemical used, and have low energy requirements.¹⁴⁸ In effort to meet these requirements,

824 they created an organic-inorganic hybrid through biomimetic silification process in water.¹⁴⁸

825 The mechanism for sorption kinetics was determined using the batch method. The authors state

826 that the sorption mechanism is directed by electrostatic attractions between the negatively

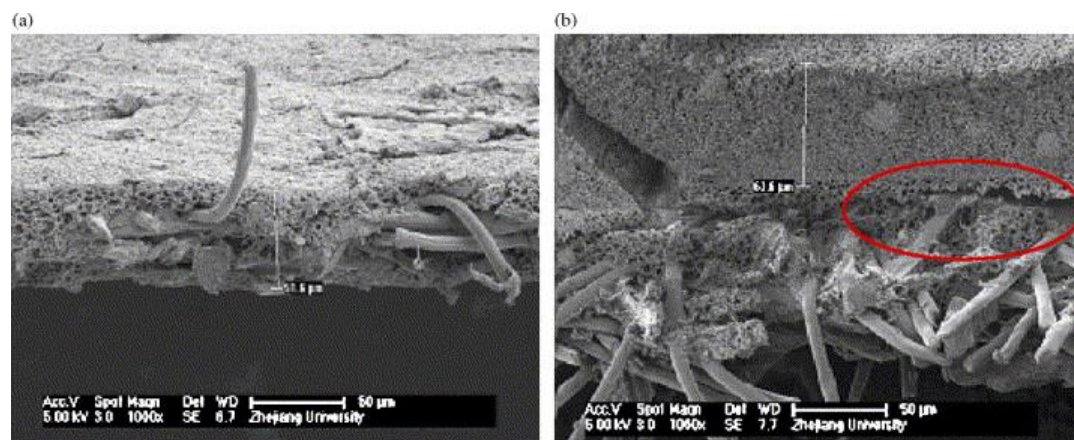
827 charged silica and positively charged metal ions.¹⁴⁸ Furthermore, the ionic radius of the cation is

828 correlated to the sorption rate of the metal on the silica.¹⁴⁸ With that being said, the larger the

829 ionic radius, the less likely it will remain solvated to compete with the silanols.¹⁴⁹ Zeta potential

830 measurements were performed as a function of pH and the PEI-silica nanospheres had an
831 isoelectric point around 8 due to the presence of a protonated amino group of the polymer.¹⁴⁸
832 Sorption isotherms were calculated to study the behavior of adsorption. The PEI-silica
833 nanoparticles were compared to the polymer-free silica nanoparticles. Langmuir-type adsorption
834 occurred for all metal ions (table 5) and the PEI-silica nanoparticles performed better than the
835 polymer-free silica nanoparticles. In addition to heavy metals, the authors tested the PEI-silica
836 nanoparticles for the sorption of polycyclic aromatic hydrocarbon (PAHs). The nanomaterials
837 demonstrated success for sorption of heavy metals and PAHs through electrostatic interactions
838 and the formation of a charge transfer complex between the PAH and tertiary amino groups.¹⁴⁹
839 More tests are needed to implement these in wastewater treatment. No regenerative studies were
840 mentioned.

841 Chitosan-based porous organic-inorganic hybrid membranes supported on nylon film were
842 prepared as a proposed metal adsorbent.¹⁴⁴ The inorganic support was
843 glycidoxypopyltrimethoxysilane (GPTMS) and chitosan was used as the organic component.¹⁴⁴
844 This paper was focused on the synthesis and characterization of these organic-inorganic hybrids.
845 Figure 8 shows a cross section of the membranes.¹⁴⁴ No adsorption studies or kinetics were
846 measured in this study. A few noteworthy mentions regarding the potential application for these
847 membrane structures as adsorbents would be the use of chitosan as the organic component of
848 these hybrid structures. Chitosan is an aminopolysaccharide, (cationic polymer) produced from
849 N-deacetylation of chitin.¹⁵⁰ It has high content of amino groups ($-NH_2$) and hydroxyl groups
850 ($-OH$) which make it a good binder toward heavy metals.¹⁵⁰ The use of a membrane increases
851 the compatibility between the organic and inorganic polymers making the hybrid structure
852 stable.¹⁴⁴



853

854 Figure 8. SEM of cross-section of nylon membrane (a) and hybrid membrane imprinted with
855 15% PEG 20 000 (b). Scale bar for (a) 51.6 µm; (b) 61.6 µm (magnification: 1000).¹⁴⁴ Reprinted
856 from Ref. 144, Copyright 2015, with permission from Elsevier.

857

858 The stable organic-inorganic support and use of chitosan would make this a very good potential
859 adsorbent for heavy metal removal. Since this review is focused on inorganic nanoadsorbents
860 removing heavy metal ions from water, no further discussion will take place.

861 The use of precious metals such as Pd (II) has increased in many fields and its
862 applications include jewelry, electronics, medical devices etc. Human health risks have emerged
863 due to the ability of Pd (II) to react with proteins, DNA, thiol-containing aminos, and cause
864 cellular damage. Therefore, the release and accumulation of Pd (II) into the environment is a
865 growing concern. Awual *et al* presented a study where they demonstrated Pd (II) detection and
866 removal using a functionalized ligand immobilized nano-conjugate adsorbent based on organic-
867 inorganic combination.¹⁵¹

868 The DHDM ligand was then immobilized in mesoporous silica under vacuum creating the
869 functionalized ligand immobilized nano-conjugate adsorbent (NCA).¹⁵¹ Sorption experiments for
870 NCA were performed via single batch and multi-component methods. The effect of pH was
871 studied and the temperature was constant (refer to table 5 for details). A filtration system was
872 used to remove the sorbent from solution after each time interval. Kinetics were measured and

873 evaluated at different Pd (II) ion concentrations. NCA was reused in multiple cycles in order to
874 test the recyclability and its long-term use. The maximum adsorption for Pd (II) was at pH 1.5
875 which is considerably lower than industrial wastewater (6-9).⁶⁰ The authors noticed the
876 formation of hydroxyl and hydroxyl-chloride species when the pH was adjusted to 5.¹⁵¹ In order
877 to understand the behavior of adsorption processes occurring with NCA and Pd(II), isotherms
878 were employed. The NCA adsorption data fit well to the Langmuir isotherm which implies that
879 the interaction between the PD(II) ions and NCA is classified as monolayer coverage.¹⁵¹ The
880 presence of other ions in relation to Pd(II) adsorption onto NCA was investigated. The studies
881 included mixing Cu²⁺, Zn²⁺, Ag⁺, Al³⁺, Cd²⁺, Co²⁺, Fe³⁺, Hg²⁺, Mg²⁺, Ni²⁺, Ca²⁺, Ru³⁺ and Pt²⁺
882 with Pd(II) ions. It can be said with confidence that the Pd(II) adsorption on to the surface of
883 NCA was not affected by the presence of these ions.¹⁵¹ A solution of thiourea and HCl was used
884 to aid the process and after 10 cycles the sorption efficiency was marginally lower.¹⁵¹ This study
885 presented an organic-inorganic adsorbent, NCA, for Pd (II) detection and recovery.¹⁵¹ The
886 novelty of this adsorbent is that it can simultaneously detect and removed Pd (II) from water.
887 Regenerative and interference ion studies suggest that it could be suitable for acidic
888 environmental applications. However the versatility of this adsorbent for other metals is
889 hindered by the maximum adsorption pH value of 1.5, which is considerably lower than typical
890 wastewater conditions.

891 These next generation nanoadsorbents have increased innovation for environmental
892 remediation of heavy metals in solution. The creative design and versatility of these adsorbents
893 allow for simultaneous detection and removal for heavy metals as previously discussed.
894 According to Sanchez *et al*, the integration of organic and inorganic nanomaterials produces a
895 high level of elementary functions in a small volume.¹⁵² The general physical properties of these

896 hybrids are thermal stability, superior mechanical properties, permeability, electronic properties
897 and can be found in an excellent article published by Sanchez *et al.*¹⁵²

898 **4 Conclusions and Prospects**

899
900 Over the last decade, considerable research on the use of inorganic nanoadsorbents for
901 adsorption of heavy metals has shown great progress. The use of adsorbents addresses the need
902 for viable, simple solutions for heavy metal removal worldwide.

903 The survey of 155 articles (2004-2014) provides evidence that work is being done to remove
904 heavy metals from wastewater using inorganic nanoadsorbents. It is clear that metal oxides and
905 CNTs are the most widely studied and utilized materials as nanoadsorbents for heavy metal
906 removal in aqueous solutions. Most notably, ZnO hollow nanospheres¹²⁷ and ZnO nanoplates¹³²
907 showed complete removal of Cu (II) in aqueous solutions. Hierarchical structures such as flower-
908 like shapes of Fe₂O₃,^{46, 72, 78} titanium.¹⁰⁷ were engineered to enhance the properties of metal
909 oxides for heavy metal removal. Each of these unique hierarchical type structures demonstrated
910 enhanced adsorption capabilities when compared to non-modified nanoparticles.

911 The increased popularity of the use of polymeric nanoadsorbents to remove heavy metals
912 from solution has also shown great promise for practical industrial applications. Kumar *et al*
913 demonstrated the capabilities of synthesized Al- and Fe-doped polymeric nanocomposite,
914 PH_22_BM_A, through the dramatic and efficient loadings of fluoride (100 mg/g) and arsenic
915 (V) 40 mg/g.²⁵ The polymeric nanoadsorbent was synthesized in effort to prepare a multi-
916 functional adsorbent for water treatment.²⁵

917 One of the most important parameters of an adsorbent is the ability for regeneration and
918 reuse. This is especially important from an economic perspective when converting to large scale
919 industrial settings. Overall, the Fe_xO_x nanomaterials showed the greatest ability for regeneration.

920 Most notably, Hu *et al* was able to regenerate spent magnetite nanoparticles up to 6 cycles to
921 remove Cr (VI) from wastewater effluent.¹⁵³ The CNTs showed great potential as adsorbents for
922 a wide range of heavy metals including radioactive elements.¹⁵⁴ However, there was very limited
923 research on CNT regeneration or exhaustion. Titanium dioxide showed the most promise for
924 regeneration, particularly the work performed by Hu *et al*, where no exhaustion of the TiO₂ was
925 observed after numerous cycles in multiple metal solutions.¹¹⁴ Luo *et al* regenerated spent TiO₂
926 for 21 cycles for As (III) removal from industrial wastewater.¹¹¹ Like the CNTs, more research
927 is needed to improve the recyclability of ZnO, and polymeric nanoparticles. For future work
928 with these materials, it is important that regeneration studies be conducted so that the ability of
929 these materials to be reused is understood.

930 Despite their wide use, nanoparticles can inadvertently cause secondary pollution due to
931 their small size and “hard to separate” suspensions in aqueous solutions.¹²⁷ This inability to
932 separate can influence the mobility and bioavailability of heavy metals in the environment. This
933 can cause an increase in the toxicity of the nanomaterials and cause side effects. The next
934 generation adsorbents, organic-inorganic hybrids, are a viable solution to the limitations of the
935 use of nanoparticles. The organic-inorganic hybrid combines the properties of organic functional
936 groups and utilizes the stable inorganic supports to create a novel hybrid capable of removing
937 heavy metal ions from water. Section 3.1 provided the most recent advances of heavy metal
938 removal utilizing the novel properties of these structures.

939 Despite their limitations, inorganic nanoadsorbents have proven their applicability to
940 remove heavy metals from aqueous and real world samples. Alternative techniques to adsorption
941 include membrane filtration, chemical precipitation, electrochemical methods and ion exchange
942 but their use can become costly and cause other forms of secondary pollution. By addressing the

943 limitations of recyclability and separation, the use of nanoadsorbents for heavy metal removal is
944 a practical, simple, process. Furthermore the flexibility in design as shown through the many
945 examples of flowers, tubes, spheres and nanocomposites as well as the ability to functionalize the
946 surface of the nanoadsorbents, gives great promise for use as a global water treatment
947 technology.

948 **5 References**

- 949
- 950 1. Fu, F.; Wang, Q., Removal of heavy metal ions from wastewaters: a review. *J. Environ.*
951 *Manage.* **2011**, *92*, (3), 407-418.
- 952 2. Naser, H. A., Assessment and management of heavy metal pollution in the marine
953 environment of the Arabian Gulf: A review. *Mar Pollut Bull* **2013**, *72*, 6-13.
- 954 3. Mendoza, O. T.; Hernández, M. A. A.; Abundis, J. G.; Mundo, N. F., Geochemistry of
955 leachates from the El Fraile sulfide tailings piles in Taxco, Guerrero, southern Mexico.
956 *Environmental Geochemistry and Health* **2006**, *28*, 243-255.
- 957 4. Fu, F.; Wang, Q., Removal of heavy metal ions from wastewaters: A review. *Journal of*
958 *Environmental Management* **2011**, *92*, (3), 407-418.
- 959 5. Naser, H. A., Assessment and management of heavy metal pollution in the marine
960 environment of the Arabian Gulf: A review. *Mar Pollut Bull* **2013**, 6-13.
- 961 6. Nriagu, J. O.; Pacyna, J. M., Quantitative assessment of worldwide contamination of air,
962 water and soils by trace metals. *Nature* **1988**, *333*, (12), 134-139.
- 963 7. Wang, S.; Mulligan, C. N., Effect of natural organic matter on arsenic release from soils
964 and sediments into groundwater. *Environmental Geochemistry and Health* **2006**, *28*, 197-214.
- 965 8. Jr., G. E. B.; Foster, A. L.; Ostergren, J. D., Mineral surfaces and bioavailability of heavy
966 metals: A molecular-scale perspective. *Proc. Natl. Acad. Sci. U. S. A.* **1999**, *96*, 3388-3395.
- 967 9. Lim, S.-R.; Schoenung, J. M., Human health and ecological toxicity potentials due to
968 heavy metal content in waste electronic devices with flat panel displays. *Journal of Hazardous*
969 *Materials* **2010**, *177*, (1-3), 251-259.
- 970 10. Karlsson, K.; Viklander, M.; Scholes, L.; Revitt, M., Heavy metal concentrations and
971 toxicity in water and sediment from stormwater ponds and sedimentation tanks. *Journal of*
972 *Hazardous Materials* **2010**, *178*, (1-3), 612-618.
- 973 11. Madoni, P.; Romeo, M. G., Acute toxicity of heavy metals towards freshwater ciliated
974 protists. *Environmental pollution* **2006**, *141*, (1), 1-7.
- 975 12. Agency, U. S. E. P. Water: Drinking Water Contaminants.
976 <http://water.epa.gov/drink/contaminants/index.cfm#Inorganic> (01/07/2015),
- 977 13. Akieh, M. N.; Lahtinen, M.; Vaeisaenen, A.; Sillanpaae, M., Preparation and
978 characterization of sodium iron titanate ion exchanger and its application in heavy metal removal
979 from waste waters. *J. Hazard. Mater.* **2008**, *152*, (2), 640-647.
- 980 14. Ismail, A. A.; Mohamed, R. M.; Ibrahim, I. A.; Kini, G.; Koopman, B., Synthesis,
981 optimization and characterization of zeolite A and its ion-exchange properties. *Colloids Surf., A*
982 **2010**, *366*, (1-3), 80-87.
- 983 15. Qiu, W.; Zheng, Y., Removal of lead, copper, nickel, cobalt, and zinc from water by a
984 cancrinite-type zeolite synthesized from fly ash. *Chem. Eng. J. (Amsterdam, Neth.)* **2009**, *145*,
985 (3), 483-488.
- 986 16. Dialynas, E.; Diamadopoulou, E., Integration of a membrane bioreactor coupled with
987 reverse osmosis for advanced treatment of municipal wastewater. *Desalination* **2009**, *238*, (1-3),
988 302-311.
- 989 17. Mohsen-Nia, M.; Montazeri, P.; Modarress, H., Removal of Cu²⁺ and Ni²⁺ from
990 wastewater with a chelating agent and reverse osmosis processes. *Desalination* **2007**, *217*, (1-3),
991 276-281.

- 992 18. Meunier, N.; Drogui, P.; Montané, C.; Hausler, R.; Mercier, G.; Blais, J.-F., Comparison
993 between electrocoagulation and chemical precipitation for metals removal from acidic soil
994 leachate. *Journal of Hazardous Materials* **2006**, *137*, (1), 581-590.
- 995 19. Hunsom, M.; Pruksathorn, K.; Damronglerd, S.; Vergnes, H.; Duverneuil, P.,
996 Electrochemical treatment of heavy metals (Cu²⁺, Cr⁶⁺, Ni²⁺) from industrial effluent and
997 modeling of copper reduction. *Water research* **2005**, *39*, (4), 610-616.
- 998 20. Deng, Y.; Englehardt, J. D., Electrochemical oxidation for landfill leachate treatment.
999 *Waste Management* **2007**, *27*, (3), 380-388.
- 1000 21. Rana, P.; Mohan, N.; Rajagopal, C., Electrochemical removal of chromium from
1001 wastewater by using carbon aerogel electrodes. *Water research* **2004**, *38*, (12), 2811-2820.
- 1002 22. Qdais, H. A.; Moussa, H., Removal of heavy metals from wastewater by membrane
1003 processes: a comparative study. *Desalination* **2004**, *164*, (2), 105-110.
- 1004 23. Yuan, X. Z.; Meng, Y. T.; Zeng, G. M.; Fang, Y. Y.; Shi, J. G., Evaluation of tea-derived
1005 biosurfactant on removing heavy metal ions from dilute wastewater by ion flotation. *Colloids
1006 and Surfaces A: Physicochemical and Engineering Aspects* **2008**, *317*, (1-3), 256-261.
- 1007 24. Jang, M.; Chen, W.; Cannon, F. S., Preloading Hydrous Ferric Oxide into Granular
1008 Activated Carbon for Arsenic Removal. *Environmental science & technology* **2008**, *42*, (9),
1009 3369-3374.
- 1010 25. Kumar, V.; Talreja, N.; Deva, D.; Sankararamakrishnan, N.; Sharma, A.; Verma, N.,
1011 Development of bi-metal doped micro- and nano multi-functional polymeric adsorbents for the
1012 removal of fluoride and arsenic(V) from wastewater. *Desalination* **2011**, *282*, 27-38.
- 1013 26. Buergisser, C. S.; Cernik, M.; Borkovec, M.; Sticher, H., Determination of nonlinear
1014 adsorption isotherms from column experiments: an alternative to batch studies. *Environmental
1015 science & technology* **1993**, *27*, (5), 943-948.
- 1016 27. Levan, M. D.; Vermeulen, T., Binary Langmuir and Freundlich Isotherms for Ideal
1017 Adsorbed Solutions. *J Phys Chem* **1981**, *85*, 3247-3250.
- 1018 28. Giles, C. H.; MacEwan, T. H.; Nakhwa, S. N.; Smith, D., Studies in Adsorption. Part
1019 XI.* A System of Classification of Solution Adsorption Isotherms, and its Use in Diagnosis of
1020 Adsorption Mechanisms and in Measurement of Specific Surface Areas of Solids. *J. Chem. Soc.*
1021 **1960**, (0), 3973-3993.
- 1022 29. Dada, A. O.; Olalekan, A. P.; Olatunya, A. M.; Dada, O., Langmuir, Freundlich, Temkin
1023 and Dubinin-Radushkevich Isotherms Studies of Equilibrium Sorption of Zn²⁺ Unto Phosphoric
1024 Acid Modified Rice Husk. *IOSR Journal of Applied Chemistry* **2012**, *3*, (1), 38-45.
- 1025 30. Karami, H., Heavy metal removal from water by magnetite nanorods. *Chem. Eng. J.*
1026 *(Amsterdam, Neth.)* **2013**, *219*, 209-216.
- 1027 31. Bailey, S. E.; Olin, T. J.; Bricka, R. M.; Adrian, D. D., A Review of Potentially Low-
1028 Cost Sorbents for Heavy Metals. *Water research* **1999**, *33*, (11), 2469-2479.
- 1029 32. Arshadi, M.; Soleymanzadeh, M.; Salvacion, J. W. L.; SalimiVahid, F., Nanoscale Zero-
1030 Valent Iron (NZVI) supported on sinoguelas waste for Pb(II) removal from aqueous solution:
1031 Kinetics, thermodynamic and mechanism. *J. Colloid Interface Sci.* **2014**, *426*, 241-251.
- 1032 33. Cheng, Z.; Gao, Z.; Ma, W.; Sun, Q.; Wang, B.; Wang, X., Preparation of magnetic
1033 Fe₃O₄ particles modified sawdust as the adsorbent to remove strontium ions. *Chem. Eng. J.*
1034 *(Amsterdam, Neth.)* **2012**, *209*, 451-457.
- 1035 34. Gupta, V. K.; Ali, I., Removal of lead and chromium from wastewater using bagasse fly
1036 ash-a sugar industry waste. *J. Colloid Interface Sci.* **2004**, *271*, (2), 321-328.

- 1037 35. Hamadi, N. K.; Chen, X. D.; Farid, M. M.; Lu, M. G. Q., Adsorption kinetics for the
1038 removal of chromium(VI) from aqueous solution by adsorbents derived from used tires and
1039 sawdust. *Chem. Eng. J. (Amsterdam, Neth.)* **2001**, *84*, (2), 95-105.
- 1040 36. Kumar, R.; Bishnoi, N. R.; Garima; Bishnoi, K., Biosorption of chromium(VI) from
1041 aqueous solution and electroplating wastewater using fungal biomass. *Chem. Eng. J.*
1042 *(Amsterdam, Neth.)* **2008**, *135*, (3), 202-208.
- 1043 37. Phuengprasop, T.; Sittiwong, J.; Unob, F., Removal of heavy metal ions by iron oxide
1044 coated sewage sludge. *J. Hazard. Mater.* **2011**, *186*, (1), 502-507.
- 1045 38. Rao, M. M.; Reddy, D. H. K. K.; Venkateswarlu, P.; Seshaiiah, K., Removal of mercury
1046 from aqueous solutions using activated carbon prepared from agricultural by-product/waste. *J*
1047 *Environ Manage* **2009**, *90*, (1), 634-43.
- 1048 39. Srivastava, V. C.; Mall, I. D.; Mishra, I. M., Adsorption thermodynamics and isosteric
1049 heat of adsorption of toxic metal ions onto bagasse fly ash (BFA) and rice husk ash (RHA).
1050 *Chem. Eng. J. (Amsterdam, Neth.)* **2007**, *132*, (1-3), 267-278.
- 1051 40. Garg, U. K.; Kaur, M. P.; Garg, V. K.; Sud, D., Removal of hexavalent chromium from
1052 aqueous solution by agricultural waste biomass. *J. Hazard. Mater.* **2007**, *140*, (1-2), 60-68.
- 1053 41. Mohan, D.; Singh, K. P.; Singh, V. K., Removal of hexavalent chromium from aqueous
1054 solution using low-cost activated carbons derived from agricultural waste materials and activated
1055 carbon fabric cloth. *Ind. Eng. Chem. Res.* **2005**, *44*, (4), 1027-1042.
- 1056 42. Kurniawan, T. A.; Sillanpää, M. E. T.; Sillanpää, M., Nanoadsorbents for Remediation of
1057 Aquatic Environment: Local and Practical Solutions for Global Water Pollution Problems. *Crit.*
1058 *Rev. Environ. Sci. Technol.* **2012**, *42*, 1233-1295.
- 1059 43. Savage, N.; Diallo, M., Nanomaterials and Water Purification: Opportunities and
1060 Challenges. *Journal of Nanoparticle Research* **2005**, *7*, (4-5), 331-342.
- 1061 44. Ge, F.; Li, M.-M.; Ye, H.; Zhao, B.-X., Effective removal of heavy metal ions Cd²⁺,
1062 Zn²⁺, Pb²⁺, Cu²⁺ from aqueous solution by polymer-modified magnetic nanoparticles. *J.*
1063 *Hazard. Mater.* **2012**, *211-212*, 366-372.
- 1064 45. Wang, H.; Chen, Q.-W.; Chen, J.; Yu, B.-X.; Hu, X.-Y., Carboxyl and negative charge-
1065 functionalized superparamagnetic nanochains with amorphous carbon shell and magnetic core:
1066 synthesis and their application in removal of heavy metal ions. *Nanoscale* **2011**, *3*, (11), 4600-3.
- 1067 46. Cao, C.-Y.; Qu, J.; Yan, W.-S.; Zhu, J.-F.; Wu, Z.-Y.; Song, W.-G., Low-Cost Synthesis
1068 of Flowerlike α -Fe₂O₃ Nanostructures for Heavy Metal Ion Removal: Adsorption Property and
1069 Mechanism. *Langmuir* **2012**, *28*, (9), 4573-4579.
- 1070 47. Cheng, X.-L.; Jiang, J.-S.; Jin, C.-Y.; Lin, C.-C.; Zeng, Y.; Zhang, Q.-H., Cauliflower-
1071 like α -Fe₂O₃ microstructures: Toluene–water interfaceassisted synthesis, characterization, and
1072 applications in wastewater treatment and visible-light photocatalysis. *Chem Eng J* **2014**, *236*,
1073 139-148.
- 1074 48. Roy, A.; Bhattacharya, J., Removal of Cu(II), Zn(II) and Pb(II) from water using
1075 microwave-assisted synthesized maghemite nanotubes. *Chemical Engineering Journal* **2012**,
1076 *211-212*, 493-500.
- 1077 49. Badruddoza, A. Z. M.; Bin Zakir Shawon, Z.; Rahman, M. T.; Hao, K. W.; Hidajat, K.;
1078 Uddin, M. S., Ionically modified magnetic nanomaterials for arsenic and chromium removal
1079 from water. *Chem. Eng. J. (Amsterdam, Neth.)* **2013**, *225*, 607-615.
- 1080 50. Lei, Y.; Chen, F.; Luo, Y.; Zhang, L., Three-dimensional magnetic graphene oxide
1081 foam/Fe₃O₄ nanocomposite as an efficient absorbent for Cr(VI) removal. *J. Mater. Sci.* **2014**,
1082 *49*, (12), 4236-4245.

- 1083 51. Tan, L.; Xu, J.; Xue, X.; Lou, Z.; Zhu, J.; Baig, S. A.; Xu, X., Multifunctional
1084 nanocomposite Fe₃O₄@SiO₂-mPD/SP for selective removal of Pb(II) and Cr(VI) from aqueous
1085 solutions. *RSC Adv.* **2014**, *4*, (86), 45920-45929.
- 1086 52. Ngomsik, A.-F.; Bee, A.; Talbot, D.; Cote, G., Magnetic solid-liquid extraction of
1087 Eu(III), La(III), Ni(II) and Co(II) with maghemite nanoparticles. *Sep. Purif. Technol.* **2012**, *86*,
1088 1-8.
- 1089 53. Shipley, H.; Yean, S.; Kan, A.; Tomson, M., A sorption kinetics model for arsenic
1090 adsorption to magnetite nanoparticles. *Environ Sci Pollut Res* **2010**, *17*, (5), 1053-1062.
- 1091 54. Roy, A.; Bhattacharya, J., A binary and ternary adsorption study of wastewater Cd(II),
1092 Ni(II) and Co(II) by γ -Fe₂O₃ nanotubes. *Sep. Purif. Technol.* **2013**, *115*, 172-179.
- 1093 55. Karami, H.; Chidar, E., Pulsed-electrochemical synthesis and characterizations of
1094 magnetite nanorods. *Int. J. Electrochem. Sci.* **2012**, *7*, 2077-2090.
- 1095 56. Warner, C. L.; Addleman, R. S.; Cinson, A. D.; Droubay, T. C.; Engelhard, M. H.; Nash,
1096 M. A.; Yantasee, W.; Warner, M. G., High-Performance, Superparamagnetic, Nanoparticle-
1097 Based Heavy Metal Sorbents for Removal of Contaminants from Natural Waters. *ChemSusChem*
1098 **2010**, *3*, (6), 749-757.
- 1099 57. Sun, S.; Zeng, H.; Robinson, D. B.; Raoux, S.; Rice, P. M.; Wang, S. X.; Li, G.,
1100 Monodisperse MFe₂O₄ (M = Fe, Co, Mn) Nanoparticles. *JACS* **2003**, *126*, 273-279.
- 1101 58. Kang, Y. S.; Rishud, S.; Rabolt, J. F.; Stroeve, P., Synthesis and characterization of
1102 nanoparticle-size Fe₃O₄ and γ -Fe₂O₃ particles. *Chem Mater* **1996**, *8*, 2209-2211.
- 1103 59. Hu, J.; Chen, G.; Lo, I. M. C., Removal and recovery of Cr(VI) from wastewater by
1104 maghemite nanoparticles. *Water Res.* **2005**, *39*, (18), 4528-4536.
- 1105 60. Acheampong, M. A.; Meulepasa, R. J. W.; Lens, P. N. L., Removal of heavymetals and
1106 cyanide from gold mine wastewater. *J Chem Technol Biotechnol* **2009**, *85*, 590-613.
- 1107 61. Qi, X.; Li, N.; Xu, Q.; Chen, D.; Li, H.; Lu, J., Water-soluble Fe₃O₄ superparamagnetic
1108 nanocomposites for the removal of low concentration mercury(II) ions from water. *RSC Adv.*
1109 **2014**, *4*, (88), 47643-47648.
- 1110 62. Khaydarov, R. A.; Khaydarov, R. R.; Gapurova, O., Water purification from metal ions
1111 using carbon nanoparticle-conjugated polymer nanocomposites. *Water Res.* **2010**, *44*, (6), 1927-
1112 1933.
- 1113 63. Park, J.; An, K.; Hwang, Y.; Park, J.-G.; Noh, H.-J.; Kim, J.-Y.; Park, J.-H.; Hwang, N.-
1114 M.; Hyeon, T., Ultra-large-scale syntheses of monodisperse nanocrystals. *Nature Materials*
1115 **2004**, *3*, 891-895.
- 1116 64. Jiang, J.; Gu, H.; Shao, H.; Devlin, E.; Papaefthymiou, G. C.; Ying, J. Y., Bifunctional
1117 Fe₃O₄-Ag Heterodimer Nanoparticles for Two-Photon Fluorescence Imaging and Magnetic
1118 Manipulation. *Advanced Materials* **2008**, *20*, (23), 4403-4407.
- 1119 65. Feitoza, N. C.; Goncalves, T. D.; Mesquita, J. J.; Menegucci, J. S.; Santos, M.-K. M. S.;
1120 Chaker, J. A.; Cunha, R. B.; Medeiros, A. M. M.; Rubim, J. C.; Sousa, M. H., Fabrication of
1121 glycine-functionalized maghemite nanoparticles for magnetic removal of copper from
1122 wastewater. *J. Hazard. Mater.* **2014**, *264*, 153-160.
- 1123 66. Hanif, S.; Shahzad, A., Removal of chromium(VI) and dye Alizarin Red S (ARS) using
1124 polymer-coated iron oxide (Fe₃O₄) magnetic nanoparticles by co-precipitation method. *J.*
1125 *Nanopart. Res.* **2014**, *16*, (6), 1-15.
- 1126 67. He, F.; Wang, W.; Moon, J.-W.; Howe, J.; Pierce, E. M.; Liang, L., Rapid removal of
1127 Hg(II) from aqueous solutions using thiol-functionalized Zn-doped biomagnetite particles. *ACS*
1128 *Appl. Mater. Interfaces* **2012**, *4*, (8), 4373-4379.

- 1129 68. Yong-Mei, H.; Man, C.; Zhong-Bo, H., Effective removal of Cu (II) ions from aqueous
1130 solution by amino-functionalized magnetic nanoparticles. *J Hazard Mater* **2010**, *184*, 392-399.
- 1131 69. Liu, J.-f.; Zhao, Z.-s.; Jiang, G.-b., Coating Fe₃O₄ Magnetic Nanoparticles with Humic
1132 Acid for High Efficient Removal of Heavy Metals in Water. *Environ. Sci. Technol.* **2008**, *42*,
1133 (18), 6949-6954.
- 1134 70. Yantasee, W.; Warner, C. L.; Sangvanich, T.; Addleman, R. S.; Carter, T. G.; Wiacek, R.
1135 J.; Fryxell, G. E.; Timchalk, C.; Warner, M. G., Removal of Heavy Metals from Aqueous
1136 Systems with Thiol Functionalized Superparamagnetic Nanoparticles. *Environ. Sci. Technol.*
1137 **2007**, *41*, (14), 5114-5119.
- 1138 71. Song, J.; Kong, H.; Jang, J., Adsorption of heavy metal ions from aqueous solution by
1139 polyrhodanine-encapsulated magnetic nanoparticles. *Journal of colloid and interface science*
1140 **2011**, *359*, (2), 505-11.
- 1141 72. Liang, H.; Xu, B.; Wang, Z., Self-assembled 3D flower-like α -Fe₂O₃ microstructures
1142 and their superior capability for heavy metal ion removal. *Mater. Chem. Phys.* **2013**, *141*, (2-3),
1143 727-734.
- 1144 73. Shipley, H.; Engates, K.; Grover, V., Removal of Pb(II), Cd(II), Cu(II), and Zn(II) by
1145 hematite nanoparticles: effect of sorbent concentration, pH, temperature, and exhaustion.
1146 *Environ Sci Pollut Res* **2013**, *20*, (3), 1727-1736.
- 1147 74. Grover, V. A.; Hu, J.; Engates, K. E.; Shipley, H. J., Adsorption and desorption of
1148 bivalent metals to hematite nanoparticles. *Environmental Toxicology and Chemistry* **2012**, *31*,
1149 (1), 86-92.
- 1150 75. Koo, H. Y.; Lee, H.-J.; Go, H.-A.; Lee, Y. B.; Bae, T. S.; Kim, J. K.; Choi, W. S.,
1151 Graphene-Based Multifunctional Iron Oxide Nanosheets with Tunable Properties. *Chem. - Eur.*
1152 *J.* **2011**, *17*, (4), 1214-1219, S1214/1-S1214/10.
- 1153 76. Fei, J.; Cui, Y.; Zhao, J.; Gao, L.; Yang, Y.; Li, J., Large-scale preparation of 3D self-
1154 assembled iron hydroxide and oxide hierarchical nanostructures and their applications for water
1155 treatment. *Journal of Materials Chemistry* **2011**, *21*, (32), 11742-11746.
- 1156 77. Zhong, L.-S.; Hu, J.-S.; Cao, A.-M.; Liu, Q.; Song, W.-G.; Wan, L.-J., 3D Flowerlike
1157 Ceria Micro/Nanocomposite Structure and Its Application for Water Treatment and CO
1158 Removal. *Chem. Mater.* **2007**, *19*, (7), 1648-1655.
- 1159 78. Zhong, L.-S.; Hu, J.-S.; Liang, H.-P.; Cao, A.-M.; Song, W.-G.; Wan, L.-J., Self-
1160 Assembled 3D Flowerlike Iron Oxide Nanostructures and Their Application in Water Treatment.
1161 *Advanced Materials* *18*, 2426-2431.
- 1162 79. Giménez, J.; Martínez, M.; de Pablo, J.; Rovira, M.; Duro, L., Arsenic sorption onto
1163 natural hematite, magnetite, and goethite. *Journal of Hazardous Materials* **2007**, *141*, (3), 575-
1164 580.
- 1165 80. Jeon, B.-H.; Dempsey, B. A.; Burgos, W. D.; Royer, R. A.; Roden, E. E., Modeling the
1166 sorption kinetics of divalent metal ions to hematite. *Water research* **2004**, *38*, (10), 2499-2504.
- 1167 81. Mamindy-Pajany, Y.; Hurel, C.; Marmier, N.; Roméo, M., Arsenic (V) adsorption from
1168 aqueous solution onto goethite, hematite, magnetite and zero-valent iron: Effects of pH,
1169 concentration and reversibility. *Desalination* **2011**, *281*, (0), 93-99.
- 1170 82. Cotten, G. B.; Eldredge, H. B., Nanolevel Magnetic Separation Model Considering Flow
1171 Limitations. *Separation Science and Technology* **2002**, *37*, (16), 3755-3779.
- 1172 83. Parham, H.; Rahbar, N., Solid phase extraction–spectrophotometric determination of
1173 fluoride in water samples using magnetic iron oxide nanoparticles. *Talanta* **2009**, *80*, (2), 664-
1174 669.

- 1175 84. Di, Z.-C.; Ding, J.; Peng, X.-J.; Li, Y.-H.; Luan, Z.-K.; Liang, J., Chromium adsorption
1176 by aligned carbon nanotubes supported ceria nanoparticles. *Chemosphere* **2006**, *62*, 861-865.
- 1177 85. Zhang, Y.; Yang, M.; Huang, X., Arsenic(V) removal with a Ce(IV)-doped iron oxide
1178 adsorbent. *Chemosphere* **2003**, *51*, (9), 945-952.
- 1179 86. Tokunaga, S.; Hardon, M. J.; Wasay, S. A., Removal of fluoride ions from aqueous
1180 solution by multivalent metal
1181 compounds. *Int. J. Environ. Studies* **1995**, *48*, (1), 17-28.
- 1182 87. Cao, A.; Zhu, H.; Zhang, X.; Li, X.; Ruan, D.; Xu, C.; Wei, B.; Liang, J., Hydrogen
1183 storage of dense-aligned carbon nanotubes. *Chem. Phys. Lett.* **2001**, *342*, 510-514.
- 1184 88. Recillas, S.; Colon, J.; Casals, E.; Gonzalez, E.; Puentes, V.; Sanchez, A.; Font, X.,
1185 Chromium VI adsorption on cerium oxide nanoparticles and morphology changes during the
1186 process. *J. Hazard. Mater.* **2010**, *184*, (1-3), 425-431.
- 1187 89. Sun, W.; Li, Q.; Gao, S.; Shang, J. K., Exceptional arsenic adsorption performance of
1188 hydrous cerium oxide nanoparticles: Part B. Integration with silica monoliths and dynamic
1189 treatment. *Chemical Engineering Journal* **2012**, *185–186*, (0), 136-143.
- 1190 90. Cao, C.-Y.; Cui, Z.-M.; Chen, C.-Q.; Song, W.-G.; Cai, W., Ceria Hollow Nanospheres
1191 Produced by a Template-Free Microwave-Assisted Hydrothermal Method for Heavy Metal Ion
1192 Removal and Catalysis. *J. Phys. Chem. C* **2010**, *114*, (21), 9865-9870.
- 1193 91. Gupta, V. K.; Agarwal, S.; Saleh, T. A., Chromium removal by combining the magnetic
1194 properties of iron oxide with adsorption properties of carbon nanotubes. *Water research* **2011**,
1195 *45*, 2207-2212.
- 1196 92. Iijima, S., Helical Microtubules of Graphitic Carbon. *Letters to Nature* **1991**, *354*, 56-58.
- 1197 93. Bottini, M.; Bruckner, S.; Nika, K.; Bottini, N.; Bellucci, S.; Magrini, A.; Bergamaschi,
1198 A.; Mustelin, T., Multi-walled carbon nanotubes induce T lymphocyte apoptosis. *Toxicology*
1199 *Letters* **2006**, *160*, (2), 121-126.
- 1200 94. Muller, J.; Huaux, F.; Lison, D., Respiratory toxicity of carbon nanotubes: How worried
1201 should we be? *Carbon* **2006**, *44*, (6), 1048-1056.
- 1202 95. Tofighy, M. A.; Mohammadi, T., Adsorption of divalent heavy metal ions from water
1203 using carbon nanotube sheets. *J. Hazard. Mater.* **2011**, *185*, (1), 140-147.
- 1204 96. Poland, C. A.; Duffin, R.; Kinloch, I.; Maynard, A.; Wallace, W. A. H.; Seaton, A.;
1205 Stone, V.; Brown, S.; MacNee, W.; Donaldson, K., Carbon nanotubes introduced into the
1206 abdominal cavity of mice show asbestos-like pathogenicity in a pilot study. *Nat Nano* **2008**, *3*,
1207 (7), 423-428.
- 1208 97. Smith, C. J.; Shaw, B. J.; Handy, R. D., Toxicity of single walled carbon nanotubes to
1209 rainbow trout, (*Oncorhynchus mykiss*): Respiratory toxicity, organ pathologies, and other
1210 physiological effects. *Aquatic Toxicology* **2007**, *82*, (2), 94-109.
- 1211 98. Rao, G. P.; Lu, C.; Su, F., Sorption of divalent metal ions from aqueous solution by
1212 carbon nanotubes: A review. *Sep. Purif. Technol.* **2007**, *58*, 224-231.
- 1213 99. Moghaddam, H. K.; Pakizeh, M., Experimental study on mercury ions removal from
1214 aqueous solution by MnO₂/CNTs nanocomposite adsorbent. *J. Ind. Eng. Chem. (Amsterdam,*
1215 *Neth.)* **2014**, Ahead of Print.
- 1216 100. Gupta, V. K.; Agarwal, S.; Saleh, T. A., Synthesis and characterization of alumina-coated
1217 carbon nanotubes and their application for lead removal. *J Hazard Mater* **2011**, *185*, 17-23.
- 1218 101. Chen, C. L.; Wang, X. K.; Nagatsu, M., Europium adsorption on multiwall carbon
1219 nanotube/iron oxide magnetic composite in the presence of polyacrylic acid. *Environmental*
1220 *science & technology* **2011**, *185*, 17-23.

- 1221 102. Debnath, S.; Ghosh, U. C., Equilibrium modeling of single and binary adsorption of
1222 Cd(II) and Cu(II) onto agglomerated nano structured titanium(IV) oxide. *Desalination* **2011**,
1223 273, (2-3), 330-342.
- 1224 103. Guan, X.; Du, J.; Meng, X.; Sun, Y.; Sun, B.; Hu, Q., Application of titanium dioxide in
1225 arsenic removal from water: A review. *J. Hazard. Mater.* **2012**, 215-216, 1-16.
- 1226 104. Bavykin, D. V.; Friedrich, J. M.; Walsh, F. C., Protonated Titanates and TiO₂
1227 Nanostructured Materials: Synthesis, Properties, and Applications. *Advanced Materials* **2006**, 18,
1228 (21), 2807-2824.
- 1229 105. Lin, C.-H.; Wong, D. S.-H.; Lu, S.-Y., Layered Protonated Titanate Nanosheets
1230 Synthesized with a Simple One-Step, Low-Temperature, Urea-Modulated Method as an
1231 Effective Pollutant Adsorbent. *ACS Appl. Mater. Interfaces* **2014**, 6, (19), 16669-16678.
- 1232 106. Yang, D.; Zheng, Z.; Liu, H.; Zhu, H.; Ke, X.; Xu, Y.; Wu, D.; Sun, Y., Layered Titanate
1233 Nanofibers as Efficient Adsorbents for Removal of Toxic Radioactive and Heavy Metal Ions
1234 from Water. *J. Phys. Chem. C* **2008**, 112, (42), 16275-16280.
- 1235 107. Huang, J.; Cao, Y.; Liu, Z.; Deng, Z.; Tang, F.; Wang, W., Efficient removal of heavy
1236 metal ions from water system by titanate nanoflowers. *Chem. Eng. J. (Amsterdam, Neth.)* **2012**,
1237 180, 75-80.
- 1238 108. Lee, Y.-C.; Yang, J.-W., Self-assembled flower-like TiO₂ on exfoliated graphite oxide
1239 for heavy metal removal. *J. Ind. Eng. Chem. (Amsterdam, Neth.)* **2012**, 18, (3), 1178-1185.
- 1240 109. Byrne, H. E.; Mazyck, D. W., Removal of trace level aqueous mercury by adsorption and
1241 photocatalysis on silica-titania composites. *J. Hazard. Mater.* **2009**, 170, (2-3), 915-919.
- 1242 110. Sharma, A.; Lee, B.-K., Cd(II) removal and recovery enhancement by using acrylamide-
1243 titanium nanocomposite as an adsorbent. *Appl Sur Sci* **2014**, 313, 624-632.
- 1244 111. Luo, T.; Cui, J.; Hu, S.; Huang, Y.; Jing, C., Arsenic Removal and Recovery from
1245 Copper Smelting Wastewater Using TiO₂. *Environmental science & technology* **2010**, 44, (23),
1246 9094-9098.
- 1247 112. Pena, M.; Meng, X.; Korfiatis, G. P.; Jing, C., Adsorption Mechanism of Arsenic on
1248 Nanocrystalline Titanium Dioxide. *Environmental science & technology* **2006**, 40, (4), 1257-
1249 1262.
- 1250 113. Engates, K. E.; Shipley, H. J., Adsorption of Pb, Cd, Cu, Zn, and Ni to titanium dioxide
1251 nanoparticles: effect of particle size, solid concentration, and exhaustion. *Environ. Sci. Pollut.*
1252 *Res.* **2011**, 18, (3), 386-395.
- 1253 114. Hu, J.; Shipley, H., Regeneration of spent TiO₂ nanoparticles for Pb (II), Cu (II), and Zn
1254 (II) removal. *Environ Sci Pollut Res* **2013**, 20, (8), 5125-5137.
- 1255 115. Rafatullah, M.; Sulaiman, O.; Hashim, R.; Ahmad, A., Adsorption of copper (II),
1256 chromium (III), nickel (II) and lead (II) ions from aqueous solutions by meranti sawdust. *Journal*
1257 *of Hazardous Materials* **2009**, 170, (2-3), 969-977.
- 1258 116. Yang, D. J.; Zheng, Z. F.; Zhu, H. Y.; Liu, H. W.; Gao, X. P., Titanate Nanofibers as
1259 Intelligent Absorbents for the Removal of Radioactive Ions from Water. *Advanced Materials*
1260 **2008**, 20, (14), 2777-2781.
- 1261 117. Bancroft, G. M.; Metson, J. B.; Kanetkar, S. M.; Brown, J. D., Surface studies on a
1262 leached sphene glass. *Nature* **1982**, 299, 708-710.
- 1263 118. Tang, Y.; Gong, D.; Lai, Y.; Shen, Y.; Zhang, Y.; Huang, Y.; Tao, J.; Lin, C.; Dong, Z.;
1264 Chen, Z., Hierarchical layered titanate microspherulite: formation by electrochemical spark
1265 discharge spallation and application in aqueous pollutant treatment. *Journal of Materials*
1266 *Chemistry* **2010**, 20, (45), 10169-10178.

- 1267 119. Sharma, A. K.; Lee, B.-K., Lead sorption onto acrylamide modified titanium
1268 nanocomposite from aqueous media. *Journal of Environmental Management* **2013**, *128*, (0),
1269 787-797.
- 1270 120. Yang, K.; Xing, B., Sorption of Phenanthrene by Humic Acid-Coated Nanosized TiO₂
1271 and ZnO. *Environmental science & technology* **2009**, *43*, (6), 1845-1851.
- 1272 121. Chen, Q.; Yin, D.; Zhu, S.; Hu, X., Adsorption of cadmium(II) on humic acid coated
1273 titanium dioxide. *Journal of colloid and interface science* **2012**, *367*, 241-248.
- 1274 122. Aguado, J.; van Grieken, R.; López-Muñoz, M.-J.; Marugán, J., A comprehensive study
1275 of the synthesis, characterization and activity of TiO₂ and mixed TiO₂/SiO₂ photocatalysts.
1276 *Applied Catalysis A: General* **2006**, *312*, (0), 202-212.
- 1277 123. Magrez, A.; Horváth, L.; Smajda, R.; Salicio, V.; Pasquier, N.; Forró, L.; Schwaller, B.,
1278 Cellular Toxicity of TiO₂-Based Nanofilaments. *ACS Nano* **2009**, *3*, (8), 2274-2280.
- 1279 124. Gerloff, K.; Fenoglio, I.; Carella, E.; Kolling, J.; Albrecht, C.; Boots, A. W.; Förster, I.;
1280 Schins, R. P. F., Distinctive Toxicity of TiO₂ Rutile/Anatase Mixed Phase Nanoparticles on
1281 Caco-2 Cells. *Chemical Research in Toxicology* **2012**, *25*, (3), 646-655.
- 1282 125. Zhu, X.; Zhou, J.; Cai, Z., TiO₂ Nanoparticles in the Marine Environment: Impact on the
1283 Toxicity of Tributyltin to Abalone (*Haliotis diversicolor supertexta*) Embryos. *Environmental*
1284 *science & technology* **2011**, *45*, (8), 3753-3758.
- 1285 126. Flytzani-Stephanopoulos, M.; Sakbodin, M.; Wang, Z., Regenerative Adsorption and
1286 Removal of H₂S from Hot Fuel Gas Streams by Rare Earth Oxides. *Science* **2006**, *312*, (5779),
1287 1508-1510.
- 1288 127. Wang, X.; Cai, W.; Liu, S.; Wang, G.; Wu, Z.; Zhao, H., ZnO hollow microspheres with
1289 exposed porous nanosheets surface: Structurally enhanced adsorption towards heavy metal ions.
1290 *Colloids and Surfaces A: Physicochemical and Engineering Aspects* **2013**, *422*, (0), 199-205.
- 1291 128. Sheela, T.; Nayaka, Y. A.; Viswanatha, R.; Basavanna, S.; Venkatesha, T. G., Kinetics
1292 and thermodynamics studies on the adsorption of Zn(II), Cd(II) and Hg(II) from aqueous
1293 solution using zinc oxide nanoparticles. *Powder Technology* **2012**, *217*, (0), 163-170.
- 1294 129. Erdem, E.; Karapinar, N.; Donat, R., The removal of heavy metal cations by natural
1295 zeolites. *Journal of colloid and interface science* **2004**, *280*, (2), 309-314.
- 1296 130. Salehi, R.; Arami, M.; Mahmoodi, N. M.; Bahrami, H.; Khorramfar, S., Novel
1297 biocompatible composite (Chitosan-zinc oxide nanoparticle): Preparation, characterization and
1298 dye adsorption properties. *Colloids Surf., B* **2010**, *80*, (1), 86-93.
- 1299 131. Jing, Z.; Zhan, J., Fabrication and Gas-Sensing Properties of Porous ZnO Nanoplates.
1300 *Advanced Materials* **2008**, *20*, (23), 4547-4551.
- 1301 132. Wang, X.; Cai, W.; Lin, Y.; Wang, G.; Liang, C., Mass production of
1302 micro/nanostructured porous ZnO plates and their strong structurally enhanced and selective
1303 adsorption performance for environmental remediation. *J. Mater. Chem.* **2010**, *20*, (39), 8582-
1304 8590.
- 1305 133. Ballerini, G.; Ogle, K.; Barthés-Labrousse, M. G., The acid-base properties of the surface
1306 of native zinc oxide layers: An XPS study of adsorption of 1,2-diaminoethane. *Applied Surface*
1307 *Science* **2007**, *253*, (16), 6860-6867.
- 1308 134. Ma, X.; Wang, Y.; Gao, M.; Xu, H.; Li, G., A novel strategy to prepare ZnO/PbS
1309 heterostructured functional nanocomposite utilizing the surface adsorption property of ZnO
1310 nanosheets. *Catal. Today* **2010**, *158*, (3-4), 459-463.

- 1311 135. Khan, S. B.; Rahman, M. M.; Marwani, H. M.; Asiri, A. M.; Alamry, K. A., An
1312 assessment of zinc oxide nanosheets as a selective adsorbent for cadmium. *Nanoscale Research*
1313 *Letters* **2013**, *8*, (1), 377-377.
- 1314 136. Kikuchi, Y.; Qian, Q.; Machida, M.; Tatsumoto, H., Effect of ZnO loading to activated
1315 carbon on Pb(II) adsorption from aqueous solution. *Carbon* **2005**, *44*, (2), 195-202.
- 1316 137. Amiri, O.; Emadi, H.; Hosseinpour-Mashkani, S. S. M.; Sabet, M.; Rad, M. M., Simple
1317 and surfactant free synthesis and characterization of CdS/ZnS core-shell nanoparticles and their
1318 application in the removal of heavy metals from aqueous solution. *RSC Adv.* **2014**, *4*, (21),
1319 10990-10996.
- 1320 138. Amiri, O.; Hosseinpour-Mashkani, S. M.; Mohammadi Rad, M.; Abdvali, F.,
1321 Sonochemical synthesis and characterization of CdS/ZnS core-shell nanoparticles and
1322 application in removal of heavy metals from aqueous solution. *Superlattices Microstruct.* **2014**,
1323 *66*, 67-75.
- 1324 139. Hua, M.; Zhang, S.; Pan, B.; Zhang, W.; Lv, L.; Zhang, Q., Heavy metal removal from
1325 water/wastewater by nanosized metal oxides: A review. *J Hazard Mater* **2012**, *211-212*, 317-331.
- 1326 140. Pan, B.; Pan, B.; Zhang, W.; Lv, L.; Zhang, Q.; Zheng, S., Development of polymeric
1327 and polymer-based hybrid adsorbents for pollutants removal from waters. *Chemical Engineering*
1328 *Journal* **2009**, *151*, (1-3), 19-29.
- 1329 141. Kunin, R., The use of macroreticular polymeric adsorbents for the treatment of waste
1330 effluents. *Pure Appl Chem* **1976**, *46*, 205-211.
- 1331 142. Vauthier, C.; Bouchemal, K., Methods for the Preparation and Manufacture of Polymeric
1332 Nanoparticles. *Pharm Res* **2009**, *26*, (5), 1025-1058.
- 1333 143. von Werne, T.; Patten, T. E., Preparation of Structurally Well-Defined
1334 Polymer-Nanoparticle Hybrids with Controlled/Living Radical Polymerizations. *Journal of the*
1335 *American Chemical Society* **1999**, *121*, (32), 7409-7410.
- 1336 144. Xi, F.; Wu, J.; Lin, X., Novel nylon-supported organic-inorganic hybrid membrane with
1337 hierarchical pores as a potential immobilized metal affinity adsorbent. *J. Chromatogr. A* **2006**,
1338 *1125*, (1), 38-51.
- 1339 145. Wang, C.-M.; Lee, L.-W.; Chang, T.-Y.; Chen, Y.-C.; Lin, H.-M.; Lu, K.-L.; Lii, K.-H.,
1340 Organic-Inorganic Hybrid Zinc Phosphate with 28-Ring Channels. *Chem. - Eur. J.* **2015**, *21*, (5),
1341 1878-1881.
- 1342 146. Moore, P. B.; Shen, J., An X-ray structural study of cacoxenite, a mineral phosphate.
1343 *Nature* **1983**, *306*, 356-357.
- 1344 147. Davis, M. E.; Saldarriaga, C.; Montes, C.; Garces, J.; Crowdert, C., A molecular sieve
1345 with eighteen-membered rings. *Nature* **1988**, *331*, 698-699.
- 1346 148. Arkas, M.; Tsiourvas, D., Organic/inorganic hybrid nanospheres based on hyperbranched
1347 poly(ethylene imine) encapsulated into silica for the sorption of toxic metal ions and polycyclic
1348 aromatic hydrocarbons from water. *J. Hazard. Mater.* **2009**, *170*, (1), 35-42.
- 1349 149. Silva, L. C. C. d.; Santos, L. B. O. d.; Abate, G.; Cosentino, I. C.; Fantini, M. C. A.;
1350 Masini, J. C.; Matos, J. R., Adsorption of Pb²⁺, Cu²⁺ and Cd²⁺ in FDU-1 silica and FDU-1
1351 silica modified with humic acid. *Microporous and Mesoporous Materials* **2008**, *110*, 250-259.
- 1352 150. Lazaridis, N. K.; Kyzas, G. Z.; Vassiliou, A. A.; Bikiaris, D. N., Chitosan Derivatives as
1353 Biosorbents for Basic Dyes. *Langmuir* **2007**, *23*, 7634-7643.
- 1354 151. Awual, M. R.; Hasan, M. M.; Znad, H., Organic-inorganic based nano-conjugate
1355 adsorbent for selective palladium(II) detection, separation and recovery. *Chem. Eng. J.*
1356 *(Amsterdam, Neth.)* **2015**, *259*, 611-619.

- 1357 152. Sanchez, C.; Julian, B.; Belleville, P.; Popall, M., Applications of hybrid organic-
1358 inorganic nanocomposites. *Journal of Materials Chemistry* **2005**, *15*, (35-36), 3559-3592.
- 1359 153. Hu, H.; Wang, Z.; Pan, L., Synthesis of monodisperse Fe₃O₄@silica core-shell
1360 microspheres and their application for removal of heavy metal ions from water. *J. Alloys Compd.*
1361 **2009**, *492*, (1-2), 656-661.
- 1362 154. Shao, D.; Hu, J.; Wang, X., Plasma induced grafting multiwalled carbon nanotube with
1363 chitosan and its application for removal of UO₂²⁺, Cu²⁺, and Pb²⁺ from aqueous solutions.
1364 *Plasma Processes Polym.* **2010**, *7*, (12), 977-985.
- 1365
- 1366

Tables

Table 1 Fe₃O₄ Nanoadsorbents used for Heavy metal removal

	Shape and size (nm)	Surface Area (m ² /g)	Optimal pH	Magnetic Saturation (emu/g)	Targeted Heavy metals	Isotherm model or sorption capacity	Performance	Regenerative/Number of cycles	Sample Matrix	Ref
Iron Oxide-Magnetite (Fe₃O₄) and Maghemite (γ-Fe₂O₃)										
Fe ₃ O ₄ nanoparticle	spheres; 19.3	60	8	–	As (V) As (III)	Langmuir q _m (mg/g)	1.19 1.13	–	groundwater and spiked tap water	53
γ-Fe ₂ O ₃	spheres; 10	178	2.5	3.3	Cr (VI)	Freundlich q _e (mg/g)	19.2	yes/6	effluent from metal processing plant	59
Fe ₃ O ₄ nanorods	rods; 55-65, length 900-1000		5.5	89	Fe(II) Pb(II) Zn(II) Ni(II) Cd(II) Cu(II)	Langmuir (mg/g)	127.01 112.86 107.27 95.42 88.39 79.1	yes/5	metal ions from aqueous solution	30
Fe ₃ O ₄ -MSPNPs	spheres; 13	–	7	N/A	Hg (II)	Langmuir (mg/g)	36.495	yes/3	metal ions from aqueous solution and spiked Jinji Lake water	61
Fe ₃ O ₄ -MBA	spheres; 7.9 ± 1.2	108	7.8	59.8	Co, Cu, Ag, Cd, Hg, Pb, Tl	Sorbent efficiency (10 ⁵ L/S)	Pb>Cu>Ag>Co, Cd>Hg>Tl	–	Spiked Colombia River water	56
Fe ₃ O ₄ -GSH	spheres; 7.7 ± 1.3	111.6		47.4			Pb>Hg>Cu>Ag>Cd>Co>Tl			
Fe ₃ O ₄ -PEG-SH	spheres; 8.2 ± 1.4	86.33		62.5			Pb>Cu>Hg>Ag>Cd>Co>Tl			
Fe ₃ O ₄ -DMSA	spheres; 7.2 ± 2	114		53.8			Hg>Pb>Ag>Cu>Tl>Cd>Co			
Fe ₃ O ₄ -EDTA	spheres; 8.2 ± 1.3	106.8		66			Hg, Pb, Ag>Cu, Co, Tl>Cd			

Fe ₃ O ₄ @APS@AA-co-CA	spheres; 15-20	–	5.5	52	Cd(II)	Langmuir (mg/g)	29.6	yes/4	metal ions from aqueous solution	44
					Zn(II)		43.4			
					Pb(II)		166.1			
					Cu(II)		126.9			
γ-Fe ₂ O ₃ nanotubes	tubes; 10–15, length 150-250	321.638	6	68.7	Cu(II)	Langmuir (mg/g)	111.11	–	metal ions from aqueous solution	48
					Zn(II)		84.95			
					Pb(II)		71.42			
Iron oxide-hematite (α-Fe₂O₃)										
3D flower-like α-Fe ₂ O ₃	flower-like; 5000-7000	–	12.7	N/A	As (V)	Langmuir (mg/g)	41.46	–	metal ions from aqueous solution	72
					Cr (VI)		33.82			
hematite nanoparticles	spheres; 37.0	31.7	6 and 8.0	N/A	Pb (II)	Freundlich q _e (mg/g)	3.11	yes/4	metal ions from aqueous solution, spiked San Antonio tap water	73
					Cd (II)		0.51			
					Cu(II)		0.051			
					Zn (II)		0.31			
Cauliflower-like α-Fe ₂ O ₃	cauliflower-like; 340-500	31.57	3	N/A	Cr (VI)	Langmuir q _m (mg/g)	17.27	–	metal ions from aqueous solution	47
					Pb (II)		32.54			

Table 2 CNT Nanoadsorbents used for Heavy metal removal

Type of Nanoadsorbent	Shape and size	Length (μm)	Surface Area (m^2/g)	Optimal pH	Targeted Heavy metals	Isotherm Model (best fit)	performance	Regenerative?	Sample Matrix	Ref
CeO ₂ /ACNT	tubes; 20-80 nm; ceria 20 nm	200		7	Cr (VI)	Langmuir q_m (mg/g)	31.55	-	metal ions from aqueous solution	84
MWCNT/nano-iron oxide	tubes; o.d. 30-50 nm; iron oxide 18 nm	10 to 20	92	7	Cr (III)	-	90 % adsorption after 60 min contact time	-	metal ions from aqueous solution	91

Table 3 Metal Oxide Nanoadsorbents used for Heavy metal removal

Type of Nanoadsorbent	Shape and size	Surface area (m ² /g)	Optimal pH	Targeted Heavy metals	Isotherm Model or sorption capacity	Performance	Regenerative?/# of cycles	Sample Matrix	Ref
TiO₂/Titania									
TiO ₂	-	196	6 to 7	As(III)	-	Decrease from 3310mg/L to 27 µg/L	yes/21 cycles	Wastewater from copper smelting plant	111
TiO ₂ nanoparticles	spheres; 8.3 nm	185	8	Pb (II)	Langmuir q _m (mg/g)	83.04	yes/no exhaustion observed	Aqueous lab solutions/spiked tap water	113
				Cd (II)		15.19			
				Ni (II)		6.75			
Layered protonated titanate nanosheets (LPTNs) (400-7)	nanosheets; thickness 2-15 nm; interlayer distance 0.78 nm	379	5	Pb (II)	Langmuir q _m (mg/g)	366 mg/g	-	Aqueous lab solutions	105
Na ₂ Ti ₃ O ₇ -T3	nano fibers	-	Between 6 and 7	Ba (II)	Sorption saturate capacity (mg/g)	160.64	-	Aqueous lab solutions	106
				Sr (II)		55.20			
				Pb(II)		279.45			
Na _{1.5} H _{0.5} Ti ₃ O ₇ -T3(H)	nano fibers	-	Between 6 and 7	Ba (II)	Sorption saturate capacity (mg/g)	130.44	-	Aqueous lab solutions	106
				Sr (II)		49.94			
				Pb(II)		244.26			
Titanate Nanoflowers (TNF)	flowers; 600-1100 nm	290	-	Pb(II)	Langmuir q _m (mg/g)	304.3	-	Aqueous lab solutions	107
				Cd (II), Ni (II), Zn (II)		168.6, 88.05, 98.1			
Titanate Nanotubes (TNT)	tubes; Length 200 nm, outer dia. 7-10 nm	230	-	Pb(II)	Langmuir q _m (mg/g)	147.4	-	Aqueous lab solutions	107
				Cd (II), Ni (II), Zn (II)		76.76, 40.09, 44.67			
Titanate Nanowires (TNW)	wires; Length 10 µm, dia. 40-240 nm	30	-	Pb(II)	Langmuir q _m (mg/g)	106.19	-	Aqueous lab solutions	107
				Cd (II), Ni (II), Zn (II)		47.55, 24.83, 27.66			
TiO ₂ -AM	spheres; 100µm	-	8	Cd (II)	Langmuir q _m (mg/g)	323	yes/5 cycles	Aqueous lab solutions	119

silica-titania composites (STC-0.25-12)	spheres; 45-90 μm	796	4	Hg	-	90 % Hg removal after 60 minutes	-	Aqueous lab solutions	109
ZnO									
ZnO nanoparticles	spheres; 26 nm	-	5.5	Zn (II)	Langmuir q_m (mg/g)	357	-	Aqueous lab solutions	129
				Cd (II)		387			
				Hg (II)		714			
ZnO hollow microspheres	spheres; 5-20 μm Interior nanoplate pores; 10-15 nm	46	6	Pb (II)	Freundlich q_e (mg/g)	> 160	-	Aqueous lab solutions	128
			Between 4 and 6	Cu (II)	Freundlich q_e (mg/g)	> 1400			
			6	Cd (II)	Langmuir q_m (mg/g)	28.1			
ZnO Nanoplates	plates; 10-15 nm thick; pore dia. 5-20 nm	147	Between 4 and 6	Cu (II)	Freundlich q_e (mg/g)	1600	-	Aqueous lab solutions	133
ZnO Nanosheets	squares; sides 1 μm ; nanoscale thickness	-	-	Pb (II)	Removal Capacity η (mg/g)	6.7	-	Aqueous lab solutions	135
ZnO Nanosheets	Sheets; thickness 10 nm	-	5	Cd (II)	Langmuir q_m (mg/g)	99.6	-	Aqueous lab solutions	136

Table 4 Polymeric Nanoadsorbents used for Heavy metal removal

Nanoadsorbent	Shape and Size	Surface Area (m ² /g)	Optimal pH	Targeted Heavy metals	Isotherm Model	Performance	Regenerative?	Sample Matrix	Ref
Activated polymeric bead with 4g Fe salt (APH_04)	spheres; 0.8 mm	378	6-7.5	As (V)	Freundlich q _e (mg/g)	1.37	-	Aqueous lab solutions	25
				Flouride		0.19			
Activated polymeric bead with 2g each Fe and Al salt (APH_22)	spheres; 0.8 mm	292		As (V)		0.57			
				Flouride		1.77			
Activated polymeric bead with 4g Al salt (APH_40)	spheres; 0.8 mm	340		As (V)		0.86			
				Flouride		1.28			
Activated polymeric bead with 2g each Fe and Al salt-crushed (PH22BM_A)	spheres; 100 nm	764		As (V)		3.47			
				Flouride		3.03			

Table 5 Organic-Inorganic Nanoadsorbents used for Heavy metal removal

Nanoadsorbent	Shape and size	Surface area (m ² /g)	Optimal pH	Targeted Heavy metals	Isotherm Model	Max Adsorption/capacity (mg/g)	Performance	Regenerative?/ Number of cycles	Sample Matrix	Ref
Organic-Inorganic Hybrid Zinc Phosphate with 28-Ring Channels	Refer to figure 39	-	-	Co	-	1.32	22.42 % removed after 1 h	-	aqueous lab solutions	146
				Cd		7.12	63.38 % removed after 1 h			
				Hg		16.08	80.17 % removed after 1 h			
Nano-conjugate Adsorbent (NCA)	200 μm	412	1.5	Pd (II)	Langmuir q _m	213.67	Equilibrium for Pd(II) adsorption in 30 min	yes; 10	aqueous lab solutions	152
Hybrid PEI-Silica	non-porous spheres; 305 ± 76 nm	20.6	6.2	Pb(II)	Langmuir q _m	632.91	100 % sorption after 2 days	-	aqueous lab solutions	149
				Cd(II)		595.24				
				Hg (II)		389.11				